Table 1 *List of primers used for quantitative RT-PCR*

Gene name	Forward primer	Reverse primer
Expressed sequence tag, unknown (Rn.37805)	GCATATGAGCAGCAATACT	AGTCTCTGACCCTAAATGAG
Heat-shock M_r 60,000 protein 1	AGAGTTCCTCAGAGGTTGGC	CCCCAGCAGCATCCAGTAAA
Ribosomal protein S6	CACTGTGCCTCGTCGGTTGG	AACATACTGGCGGACATC
Heat-shock M_r 10,000 protein	CGGCACTCCTTTCAACCAAT	GGCGGCGTAAGTCAT
Heme oxygenase	GTCAACATGGACGCCGACTA	ACCAGCAGCCCCAAATCCT
Intercellular adhesion molecule 1	CGGGCTTCGTGATCGTGGC	GGAGGCGGGGCTTGTACCTT
Tissue inhibitor of metalloproteinase-1	AACTCCTCGCTGCGGTTCT	GGTTTCCGGTTCGCCTACAC
Solute carrier family 7	CGGCCCTCCTCACAGTACAT	CGCAGAGGCAGGCCACGAG
Glutathione S-transferase π	CCCCTGCTCTCTGCCTATG	CTGTTTACCATTGCCGTTGA
Claudin 3	CGGCTGTGCTCACCTTAGTG	AGTTCCCATCTCTCGCTTCT
Cyclin D1	GCCCTCCGTTTCTTACTTC	AGACCTCCTCTTCGCACTTC
Stearoyl-CoA desaturase 2	GGTCAGGAATATTATCCCAT	CCAACCCGTGAATCAT
Cyclophilin	TGACTTCACACGCCATAAT	AGATGCCAGGACCTGTATGC

mended by the manufacturer, and the U34A arrays were hybridized for 16 h at 40°C at constant rotation (60 rpm). After washing, the GeneChip arrays were stained with streptavidin-phycoerythrin conjugate (Molecular probes, Eugene, OR) and then scanned with a GeneArray scanner (Hewlett-Packard, Palo Alto, CA). The scanned images were processed using an Affymetrix GeneChip Analysis Suite (Version 4.0.1) to obtain the "average difference value" for each probe set. The image from each array was scaled so that the average of average difference values of all probe sets was adjusted to 1000. The values of "fold change" were obtained with normalization for all probe sets. Scaled average difference values and fold change data from each GeneChip array were exported to flat text files and used for statistical analysis. The complete set of data are available at our web site.[4]

Data Analysis. Statistical comparisons were performed on the 2000 transcripts with the highest intensity from each GeneChip array. Before clustering, the fold change values of the genes were log10 transformed. The log-transformed fold change values were filtered for presence in six or more of the seven carcinomas. Average-linkage hierarchical clustering of an uncentered Pearson correlation similarity matrix was applied with the program Cluster, and the figures were generated with the program TreeView (25). Similarities of gene expression profiles between two given carcinomas were assessed by the Pearson correlation coefficient (25).

Quantitative RT-PCR. cDNA was synthesized from total RNA with oligo $(dT)_{12-18}$ primer and Superscript II reverse transcriptase (Invitrogen). Quantitative RT-PCR analysis was performed using a iCycler iQ detection system (Bio-Rad Laboratories, Hercules, CA) with Sybr Green PCR Core Reagents (Applied Biosystems). The sequences of the primers and annealing temperature are listed in Table 1. The number of molecules of a specific gene in a sample was measured by comparing its amplification with the amplifications of standard samples that contained 10^1-10^6 copies of the gene and was normalized to that of cyclophilin (26). Fold change of the gene in a carcinoma was calculated by dividing the normalized value of the carcinoma by that of the normal control mammary duct.

Results

Histology of the Tumors Induced. All of the mammary carcinomas induced by DMBA and PhIP were diagnosed as adenocarcinomas. Four DMBA-induced and three PhIP-induced carcinomas were selected based on availability for histological and GeneChip analyses. Histological examination of these seven carcinomas, even after retrial, did not reveal special features for DMBA-induced or PhIP-induced carcinomas (data not shown).

Gene Expression Profiling of the Mammary Carcinomas. The four DMBA-induced and three PhIP-induced mammary carcinomas were analyzed by GeneChip microarrays. From the 2000 genes, a set of 1564 genes was selected for cluster analysis with the criterion that the data of each gene in the set were present in six or seven carcinomas. Hierarchical cluster analysis separated these seven carcinomas into two main branches in concordance with the carcinogens used to induce them (Fig. 1). The correlation coefficients between two of the four DMBA-induced carcinomas ranged from 0.88 to 0.95 and those between two of the three PhIP-induced carcinomas ranged from 0.78 to 0.80. The correlation coefficient between the DMBA-induced and the PhIP-induced carcinomas was 0.63. These results showed that, although the gene expression profiles of the chemically induced rat mammary carcinomas were relatively similar, distinct gene expression profiles existed in the DMBA-induced and the PhIP-induced mammary carcinomas.

Genes with Altered Expressions. Several clusters of genes showed characteristic expression patterns that highlighted differences and similarities between the DMBA-induced and PhIP-induced mammary carcinomas (*bars* in Fig. 1*A*). Clusters A1 and A2 consisted of genes down-regulated in the DMBA group while up-regulated in the PhIP group, and genes in cluster A1 were more clearly down-regulated than those in cluster A2. Of the 19 genes in cluster A1, 17 genes showed significantly lower expression levels in the DMBA group than in the PhIP group ($P < 0.01$ by Student's t test; Fig. 1*B*).

On the other hand, clusters C1, C2, and C3 consisted of genes up-regulated in the DMBA group while down-regulated in the PhIP group, and genes in cluster C3 were more clearly up-regulated than those in clusters C1 and C2. All of the 33 genes in cluster C3 showed significantly higher expression levels in the DMBA group than in the PhIP group ($P < 0.01$ by Student's t test). *Glutathione S-transferase IV* (*Gstp1*, Rn.44821), *cathepsin D*, and MHC genes were in this cluster (Fig. 1*C*).

Cluster B consisted of genes down-regulated in both the DMBA and PhIP groups, whereas cluster D consisted of genes up-regulated in both groups. Of the 83 genes in cluster B, 37 (45%) were down-regulated with fold change values >2.5 in all seven mammary carcinomas, including *tissue inhibitor of metalloproteinase-1* (*Timp1*, Rn.25754) and *transforming growth factor-β-inducible early response* gene (*Tieg*, Rn.2398). Of the 109 genes in cluster D, 68 (62%) were up-regulated with fold changes >2.5 in all seven mammary carcinomas, including *cyclin D1* (*Ccnd1*, Rn.9471) and *DNA methyltransferase* (*Dnmt1*, Rn.6955).

Confirmation of Data from GeneChip Analysis by Quantitative RT-PCR Analysis. The data obtained by the GeneChip analysis was confirmed by quantitative RT-PCR analysis of 12 genes, which were selected as those with typical expression in each cluster (Table 2). Only when fold changes in GeneChip analysis were between −1.3 and 1.6, changes in opposite directions were occasionally observed by quantitative RT-PCR analysis. Specific changes observed in clusters A1, B, C3, and D were reproducible in the quantitative RT-PCR analysis.

[4] Internet address: http://www.nce.go.jp/research/rat-genome/.

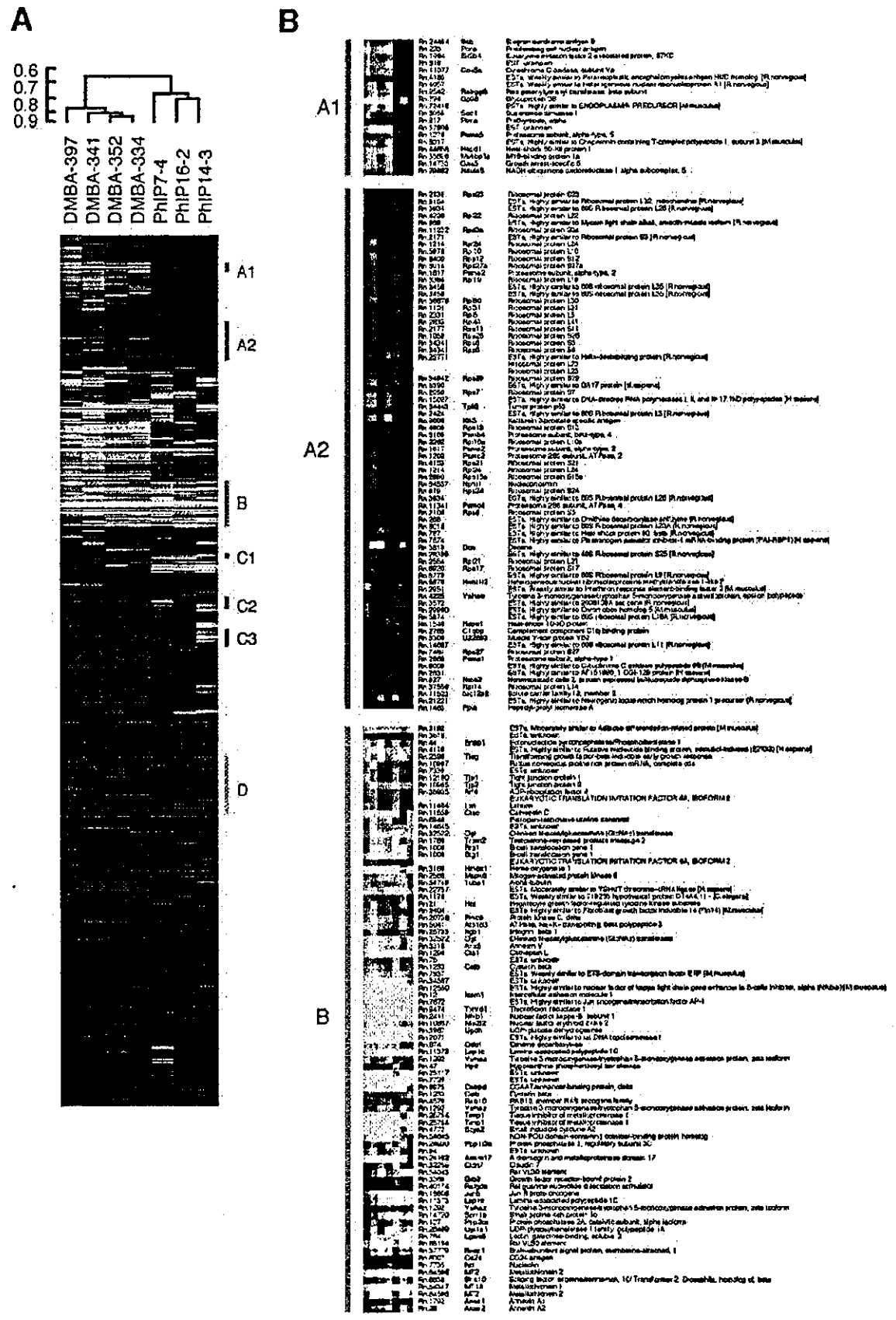
A
0.6
0.7
0.8
0.9
DMBA-397
DMBA-341
DMBA-352
DMBA-334
PhIP7-4
PhIP16-2
PhIP14-3
A1
A2
B
C1
C2
C3
D
B
A1
A2
B

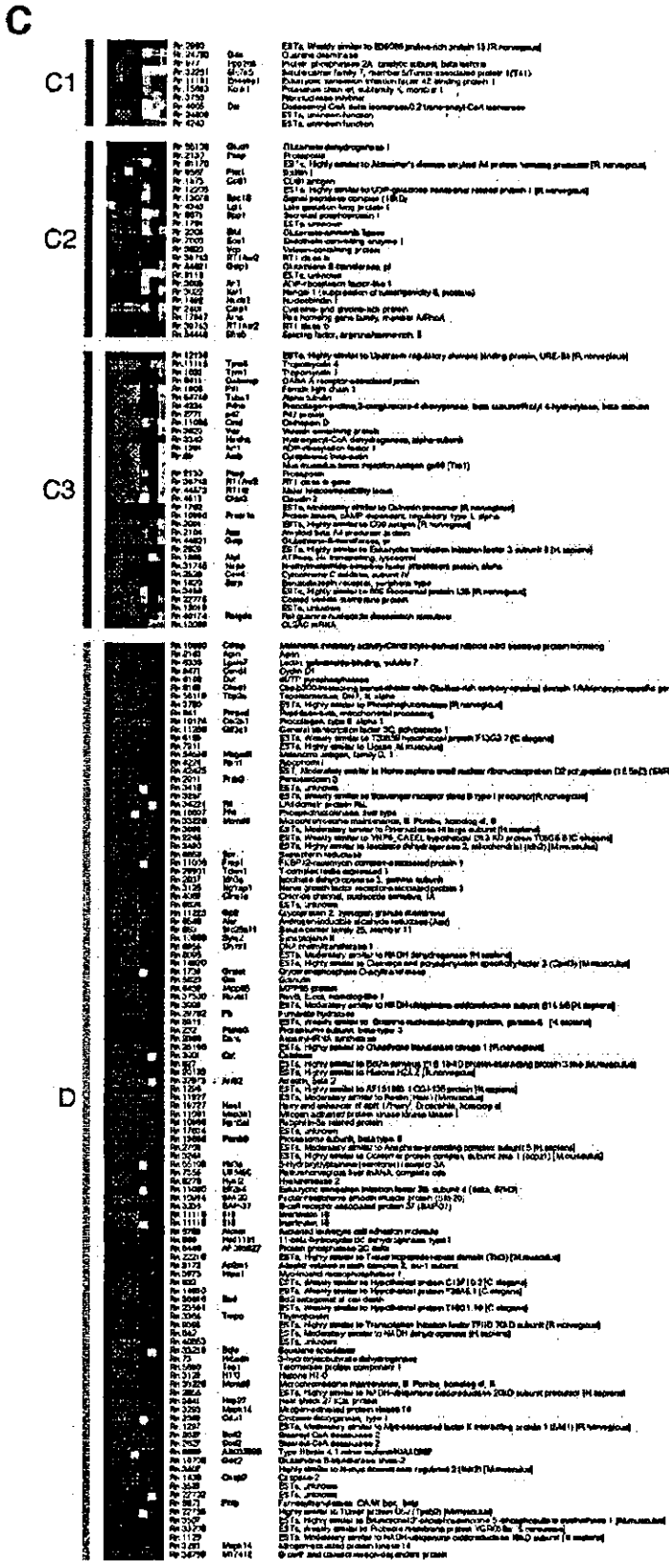

Fig. 1. *A*, Overall expression profiles of 1564 genes across the seven rat mammary carcinomas. The color scale ranged from saturated *green* (down-regulation) for log ratios −0.7 and below to saturated *red* (up-regulation) for log ratios 0.7 and above. *Black* and *gray* show unchanged expression and missing data, respectively. The *dendrogram* at the top of the *matrix* shows the degree of similarity between tumor samples. Correlation coefficients are shown to the *left*. *Bars on the side* (A1, A2, B, C1, C2, C3, and D) indicated regions with characteristic gene expression signatures. *B*, enlarged *matrices* for A1, A2, and B regions. UniGene number, locus symbol, and name of the gene are described. *C*, enlarged *matrices* for C1, C2, C3, and D regions.

Table 2 *Comparison of the data obtained by real-time RT-PCR and GeneChip analyses*

		DMBA-induced carcinomas								PhIP-induced carcinomas					
		DMBA397		DMBA341		DMBA352		DMBA334		PhIP7-4		PhIP16-2		PhIP14-3	
Cluster	Gene name	RT-PCR	Chip	RT-PCR	Chip	RT-PCR	Chip	RT-PCR	Chip	RT-PCR	Chip	RT-PCR	Chip	RT-PCR	Chip
A1	*Expressed sequence tag.* unknown (Rn.37805)	−1.4	−2.3	−4.3	−5.6	−1.7	−4.1	−2.7	−5.9	1.3	1.7	1.4	1.4	1.4	2.6
	Heat-shock M_r 60,000 protein 1	−3.7	−2.3	−5.0	−2.1	−2.1	−2.0	−3.8	−2.9	−1.6	1.5	−1.9	1.3	1.3	1.4
A2	*Ribosomal protein S6*	1.3	−1.1	−1.4	−1.3	1.7	−1.2	1.8	−1.3	−1.2	1.6	1.0	1.3	−1.1	1.2
	Heat-shock M_r 10,000 protein	−2.9	−1.7	−4.0	−1.7	−1.4	−1.5	−1.7	−2.1	2.1	1.9	1.1	1.3	2.8	2.3
B	*Heme oxygenase*	−13.5	−6.0	−23.3	−13.6	−13.6	−9.7	−17.2	−21.2	−23.0	−13.1	−149.4	−44.8	−54.1	−8.8
	Intercellular adhesion molecule 1	−6.4	−9.9	−20.6	−12.2	−14.9	−20.9	−14.3	−14.4	−19.5	−8.0	−25.7	−7.8	−34.8	−10.6
	Tissue inhibitor of metalloproteinase-1	−34.2	−6.5	−75.2	−10.0	−67.4	−14.0	−35.5	−11.2	−13.1	−5.1	−68.2	−29.2	−12.5	−4.7
C1	*Solute carrier family 7*	1.7	1.3	3.6	2.2	2.6	1.5	−1.4	1.1	−2.0	−2.0	−4.0	−2.3	−1.9	−3.5
C2	*Glutathione S-transferase π*	2.8	1.6	−1.1	1.3	3.2	1.2	4.4	2.1	−1.3	−1.0	−1.6	−1.2	−2.5	−2.1
C3	*Claudin 3*	58.1	16.0	18.4	50.1	74.1	12.8	66.0	10.6	−5.0	−3.2	−2.1	−1.4	−1.3	−9.8
D	*Cyclin D1*	75.7	10.4	29.1	23.8	62.4	16.0	22.4	23.3	5.9	3.0	25.9	15.4	13.1	13.6
	Stearoyl-CoA desaturase 2	38.5	10.8	32.1	12.0	62.0	10.9	39.0	7.9	31.5	5.7	15.5	22.9	27.2	31.6

Discussion

Expression analysis of ~8000 rat genes in four DMBA-induced and three PhIP-induced rat mammary carcinomas revealed that the carcinomas could be classified into two carcinogen-specific groups by nonbiased hierarchical analysis. Any two carcinomas within the DMBA-induced or PhIP-induced groups showed much higher correlation coefficients (>0.78) than the average among all of the carcinomas (Fig. 1). Because PhIP and a high-fat diet were used to induce carcinomas in the PhIP-induced group, the expression profile in the PhIP-induced carcinomas would reflect the combined effect of PhIP and a high-fat diet. It is known that the level of dietary fat can modulate the gene expression levels of *β-casein* and *transferrin* in the PhIP-induced mammary carcinomas (27). Histologically, all of the DMBA-induced and PhIP-induced mammary carcinomas have been diagnosed as adenocarcinomas, and even after retrial, the carcinomas could not be classified into two groups with specific etiologies. These results showed that gene expression profiles of the rat mammary carcinoma reflected their etiology that could not be estimated by histological examination. If a subset of genes that are tightly associated with specific carcinogens can be identified, the etiology of specific cancer could be retrospectively estimated from the expression profiles in it.

As for mechanisms of how expression profiles specific to DMBA- or PhIP-induced mammary carcinomas were generated, the following mechanisms can be considered. First, carcinogens are known to induce genetic alterations relatively specific to each carcinogen (28–30). These genetic alterations would affect their downstream signaling pathways, which would be reflected in the expression profiles in the resultant tumors. DMBA is known to induce A:T to T:A transversions predominantly (31), whereas PhIP induces G:C to T:A transversions and G:C deletions (24), and these differences are considered to lead to different target genes. The H-*ras* mutation frequencies and incidences of loss of heterozygosity are reported to be different between the PhIP-induced and DMBA-induced mammary carcinomas (22, 32–34). Secondly, carcinogens are known to induce specific responses in normal cells (35, 36). DMBA has a stronger effect on serum prolactin and estradiol levels than PhIP, whereas PhIP shows stronger suppression of apoptosis in the mammary glands (37). Even after repeated clonal selections during carcinogenesis, there is a possibility that some of the specific responses might be retained.

Genes differentially expressed between DMBA- and PhIP-induced mammary carcinomas are expected to be related with the molecular pathway specific to each group. Genes up-regulated in the DMBA-induced carcinomas and down-regulated in PhIP-induced carcinomas (cluster C3) included genes related to immune reactions such as a rat major histocompatibility gene and tumor rejection antigen 1 (38). This suggested that stronger immune responses were induced in the DMBA-induced carcinomas. Genes up- or down-regulated commonly in DMBA- and PhIP-induced mammary carcinomas were expected to include the genes that were related to phenotypes as mammary carcinomas. Increased expression of cyclin D1 observed in both groups was in accordance with the previous report (39).

We showed the presence of etiology-specific expression profiles in chemically induced rat mammary carcinomas. This suggested the presence of etiology-specific expression profiles in human cancers also, and this could provide clues to identifying carcinogenic agents in a certain cancer based on its gene expression profile.

References

1. Sugimura, T., Nagao, M., and Wakabayashi, K. How we should deal with unavoidable exposure of man to environmental mutagens: cooked food mutagen discovery, facts and lessons for cancer prevention. Mutat. Res., *447:* 15–25, 2000.
2. Doll, R., and Peto, R. The causes of cancer: quantitative estimates of avoidable risks of cancer in the United States today. J. Natl. Cancer Inst. (Bethesda), *66:* 1191–1308, 1981.
3. Peto, J. Cancer epidemiology in the last century and the next decade. Nature (Lond.), *411:* 390–395, 2001.
4. Hussain, S. P., and Harris, C. C. Molecular epidemiology and carcinogenesis: endogenous and exogenous carcinogens. Mutat. Res., *462:* 311–322, 2000.
5. Kakiuchi, H., Watanabe, M., Ushijima, T., Toyota, M., Imai, K., Weisburger, J. H., Sugimura, T., and Nagao, M. Specific 5′-GGGA-3′→5′-GGA-3′ mutation of the Apc gene in rat colon tumors induced by 2-amino-1-methyl-6-phenylimidazo[4,5-*b*]pyridine. Proc. Natl. Acad. Sci. USA, *92:* 910–914, 1995.
6. Liotta, L., and Petricoin, E. Molecular profiling of human cancer. Nat. Rev. Genet., *1:* 48–56, 2000.
7. Perou, C. M., Sorlie, T., Eisen, M. B., van de Rijn, M., Jeffrey, S. S., Rees, C. A., Pollack, J. R., Ross, D. T., Johnsen, H., Akslen, L. A., Fluge, O., Pergamenschikov, A., Williams, C., Zhu, S. X., Lonning, P. E., Borresen-Dale, A. L., Brown, P. O., and Botstein, D. Molecular portraits of human breast tumours. Nature (Lond.), *406:* 747–752, 2000.
8. Garber, M. E., Troyanskaya, O. G., Schluens, K., Petersen, S., Thaesler, Z., Pacyna-Gengelbach, M., van de Rijn, M., Rosen, G. D., Perou, C. M., Whyte, R. I., Altman, R. B., Brown, P. O., Botstein, D., and Petersen, I. Diversity of gene expression in adenocarcinoma of the lung. Proc. Natl. Acad. Sci. USA, *98:* 13784–13789, 2001.
9. Bhattacharjee, A., Richards, W. G., Staunton, J., Li, C., Monti, S., Vasa, P., Ladd, C., Beheshti, J., Bueno, R., Gillette, M., Loda, M., Weber, G., Mark, E. J., Lander, E. S., Wong, W., Johnson, B. E., Golub, T. R., Sugarbaker, D. J., and Meyerson, M. Classification of human lung carcinomas by mRNA expression profiling reveals distinct adenocarcinoma subclasses. Proc. Natl. Acad. Sci. USA, *98:* 13790–13795, 2001.
10. Kihara, C., Tsunoda, T., Tanaka, T., Yamana, H., Furukawa, Y., Ono, K., Kitahara, O., Zembutsu, H., Yanagawa, R., Hirata, K., Takagi, T., and Nakamura, Y. Prediction of sensitivity of esophageal tumors to adjuvant chemotherapy by cDNA microarray analysis of gene expression profiles. Cancer Res., *61:* 6474–6479, 2001.
11. Sorlie, T., Perou, C. M., Tibshirani, R., Aas, T., Geisler, S., Johnsen, H., Hastie, T., Eisen, M. B., van de Rijn, M., Jeffrey, S. S., Thorsen, T., Quist, H., Matese, J. C.,

Brown, P. O., Botstein, D., Eystein Lonning, P., and Borresen-Dale, A. L. Gene expression patterns of breast carcinomas distinguish tumor subclasses with clinical implications. Proc. Natl. Acad. Sci. USA, *98:* 10869–10874, 2001.
12. Clark, E. A., Golub, T. R., Lander, E. S., and Hynes, R. O. Genomic analysis of metastasis reveals an essential role for RhoC. Nature (Lond.), *406:* 532–535, 2000.
13. Mok, S. C., Chao, J., Skates, S., Wong, K., Yiu, G. K., Muto, M. G., Berkowitz, R. S., and Cramer, D. W. Prostasin, a potential serum marker for ovarian cancer: identification through microarray technology. J. Natl. Cancer Inst. (Bethesda), *93:* 1458–1464, 2001.
14. Hegde, P., Qi, R., Gaspard, R., Abernathy, K., Dharap, S., Earle-Hughes, J., Gay, C., Nwokekeh, N. U., Chen, T., Saeed, A. I., Sharov, V., Lee, N. H., Yeatman, T. J., and Quackenbush, J. Identification of tumor markers in models of human colorectal cancer using a 19, 200-element complementary DNA microarray. Cancer Res., *61:* 7792–7797, 2001.
15. Dhanasekaran, S. M., Barrette, T. R., Ghosh, D., Shah, R., Varambally, S., Kurachi, K., Pienta, K. J., Rubin, M. A., and Chinnaiyan, A. M. Delineation of prognostic biomarkers in prostate cancer. Nature (Lond.), *412:* 822–826, 2001.
16. Okabe, H., Satoh, S., Kato, T., Kitahara, O., Yanagawa, R., Yamaoka, Y., Tsunoda, T., Furukawa, Y., and Nakamura, Y. Genome-wide analysis of gene expression in human hepatocellular carcinomas using cDNA microarray: identification of genes involved in viral carcinogenesis and tumor progression. Cancer Res., *61:* 2129–2137, 2001.
17. Welsch, C. W. Host factors affecting the growth of carcinogen-induced rat mammary carcinomas: a review and tribute to Charles Brenton Huggins. Cancer Res., *45:* 3415–3443, 1985.
18. Hasegawa, R., Sano, M., Tamano, S., Imaida, K., Shirai, T., Nagao, M., Sugimura, T., and Ito, N. Dose-dependence of 2-amino-1-methyl-6-phenylimidazo[4,5-*b*]-pyridine (PhIP) carcinogenicity in rats. Carcinogenesis (Lond.), *14:* 2553–2557, 1993.
19. Sukumar, S., McKenzie, K., and Chen, Y. Animal models for breast cancer. Mutat. Res., *333:* 37–44, 1995.
20. Shirai, K., Uemura, Y., Fukumoto, M., Tsukamoto, T., Pascual, R., Nandi, S., and Tsubura, A. Synergistic effect of MNU and DMBA in mammary carcinogenesis and H-ras activation in female Sprague-Dawley rats. Cancer Lett., *120:* 87–93, 1997.
21. Ushijima, T., Kakiuchi, H., Makino, H., Hasegawa, R., Ishizaka, Y., Hirai, H., Yazaki, Y., Ito, N., Sugimura, T., and Nagao, M. Infrequent mutation of Ha-*ras* and *p53* in rat mammary carcinomas induced by 2-amino-1-methyl-6-phenylimidazo[4,5-*b*]pyridine. Mol. Carcinog., *10:* 38–44, 1994.
22. Kito, K., Kihana, T., Sugita, A., Murao, S., Akchi, S., Sato, M., Tachibana, M., Kimura, S., and Ueda, N. Incidence of *p53* and Ha-*ras* gene mutations in chemically induced rat mammary carcinomas. Mol. Carcinog., *17:* 78–83, 1996.
23. Sugimura, T. Overview of carcinogenic heterocyclic amines. Mutat. Res., *376:* 211–219, 1997.
24. Okochi, E., Watanabe, N., Shimada, Y., Takahashi, S., Wakazono, K., Shirai, T., Sugimura, T., Nagao, M., and Ushijima, T. Preferential induction of guanine deletion at 5′-GGGA-3′ in rat mammary glands by 2-amino-1-methyl-6-phenylimidazo[4,5-*b*]pyridine. Carcinogenesis (Lond.), *20:* 1933–1938, 1999.
25. Eisen, M. B., Spellman, P. T., Brown, P. O., and Botstein, D. Cluster analysis and display of genome-wide expression patterns. Proc. Natl. Acad. Sci. USA, *95:* 14863–14868, 1998.
26. Weisinger, G., Gavish, M., Mazurika, C., and Zinder, O. Transcription of actin, cyclophilin, and glyceraldehyde phosphate dehydrogenase genes: tissue- and treatment-specificity. Biochim. Biophys. Acta, *1446:* 225–232, 1999.
27. Roberts-Thomson, S. J., and Snyderwine, E. G. mRNA differential display of 2-amino-1-methyl-6-phenylimidazo[4,5-*b*]pyridine-induced rat mammary gland tumors. Breast Cancer Res. Treat., *51:* 99–107, 1998.
28. Yuspa, S. H., and Poirier, M. C. Chemical carcinogenesis: from animal models to molecular models in one decade. Adv. Cancer Res., *50:* 25–70, 1988.
29. Sukumar, S., and Barbacid, M. Specific patterns of oncogene activation in transplacentally induced tumors. Proc. Natl. Acad. Sci. USA, *87:* 718–722, 1990.
30. Sills, R. C., Boorman, G. A., Neal, J. E., Hong, H. L., and Devereux, T. R. Mutations in ras genes in experimental tumours of rodents. IARC Sci. Publ., *146:* 55–86, 1999.
31. Manjanatha, M. G., Shelton, S. D., Culp, S. J., Blankenship, L. R., and Casciano, D. A. DNA adduct formation and molecular analysis of *in vivo lacI* mutations in the mammary tissue of Big Blue rats treated with 7,12-dimethylbenz[*a*]anthracene. Carcinogenesis (Lond.), *21:* 265–273, 2000.
32. Hokaiwado, N., Asamoto, M., Cho, Y. M., Imaida, K., and Shirai, T. Frequent c-Ha-*ras* gene mutations in rat mammary carcinomas induced by 2-amino-1-methyl-6-phenylimidazo[4,5-*b*]pyridine. Cancer Lett., *163:* 187–190, 2001.
33. Roberts-Thomson, S. J., and Snyderwine, E. G. Effect of dietary fat on codon 12 and 13 Ha-*ras* gene mutations in 2-amino-1-methyl-6-phenylimidazo[4,5-*b*]pyridine-induced rat mammary gland tumors. Mol. Carcinog., *20:* 348–354, 1997.
34. Yu, M., Ryu, D. Y., and Snyderwine, E. G. Genomic imbalance in rat mammary gland carcinomas induced by 2-amino-1-methyl-6-phenylimidazo[4,5-*b*]pyridine. Mol. Carcinog., *27:* 76–83, 2000.
35. Bartosiewicz, M., Penn, S., and Buckpitt, A. Applications of gene arrays in environmental toxicology: fingerprints of gene regulation associated with cadmium chloride, benzo[*a*]pyrene, and trichloroethylene. Environ. Health Perspect., *109:* 71–74, 2001.
36. Afshari, C. A., Nuwaysir, E. F., and Barrett, J. C. Application of complementary DNA microarray technology to carcinogen identification, toxicology, and drug safety evaluation. Cancer Res., *59:* 4759–4760, 1999.
37. Venugopal, M., Callaway, A., and Snyderwine, E. G. 2-Amino-1-methyl-6-phenylimidazo[4,5-*b*]pyridine (PhIP) retards mammary gland involution in lactating Sprague-Dawley rats. Carcinogenesis (Lond.), *20:* 1309–1314, 1999.
38. Schild, H., and Rammensee, H. G. gp96: the immune system's Swiss army knife. Nat. Immunol., *1:* 100–101, 2000.
39. Jang, T. J., Kang, M. S., Kim, H., Kim, D. H., Lee, J. I., and Kim, J. R. Increased expression of cyclin D1, cyclin E, and p21(Cip1) associated with decreased expression of p27(Kip1) in chemically induced rat mammary carcinogenesis. Jpn. J. Cancer Res., *91:* 1222–1232, 2000.

STEM CELLS®
Original Article

The Role of PGE_2 in the Differentiation of Dendritic Cells: How Do Dendritic Cells Influence T-Cell Polarization and Chemokine Receptor Expression?

JE-JUNG LEE,[a,b] MASAO TAKEI,[c] SHINICHI HORI,[b] YOSHIKO INOUE,[d] YUKIE HARADA,[b] RYUJI TANOSAKI,[b] YOSHINOBU KANDA,[b] MASAYUKI KAMI,[b] ATSUSHI MAKIMOTO,[b] SHIN MINEISHI,[b] HIROYUKI KAWAI,[c] AKIHIRO SHIMOSAKA,[c] YUJI HEIKE,[d] YOSHINORI IKARASHI,[d] HIRO WAKASUGI,[d] YOICHI TAKAUE,[b] TAI-JU HWANG,[e] HYEOUNG-JOON KIM,[a] TADAO KAKIZOE[f]

[a]Department of Internal Medicine, Chonnam National University Medical School, Gwangju, Republic of Korea; [b]Division of Transplantation/Immunotherapy, National Cancer Center Hospital, Tokyo, Japan; [c]Kirin Brewery Company, Tokyo, Japan; [d]Pharmacology Division, Research Institute, National Cancer Center, Tokyo, Japan; [e]Department of Pediatrics, Chonnam National University Medical School, Gwangju, Republic of Korea; [f]National Cancer Center Hospital, Tokyo, Japan

Key Words. *Blood · Dendritic Cells · Th1/Th2 · Cell trafficking*

ABSTRACT

The role of prostaglandin E_2 (PGE_2) in the function of dendritic cells (DCs), T-cell polarization, and expression of chemokine receptors was evaluated in human cells. Immature DCs were generated from peripheral blood $CD14^+$ cells using a combination of GM-CSF and interleukin-4 (IL-4) with or without PGE_2. On day 6, maturation of DCs was induced by the addition of tumor necrosis factor alpha with or without PGE_2. DCs harvested on day 6 (immature DCs) or day 9 (mature DCs) were examined using functional assays. In the presence of PGE_2, immature and mature DCs showed, phenotypically, a lower expression of CD1a and, functionally, a higher allostimulatory capacity at a high DC/T-cell ratio than control cells cultured in the absence of PGE_2. DCs cultured in the presence of PGE_2 induced the differentiation of naïve T cells toward a helper T-cell type 1 (Th1) response, which was independent of IL-12 secretion in the basal state despite a slightly lower interferon gamma secretion compared with control cells. However, the function of cytotoxicity-stimulating autologous T cells was not augmented by the addition of PGE_2. Immature DCs expressed the inflammatory chemokine receptors, CCR1 and CXCR4, but not CCR6, regardless of the presence or absence of PGE_2. Mature DCs expressed CCR7 equally, measured using a migration test and the measurement of calcium flux with macrophage inflammatory protein-3β and reverse transcription-polymerase chain reaction assay in all of the groups. All of these findings suggest that PGE_2 affects the DC-promoted differentiation of naïve T cells to a Th1 response in the basal state, without affecting chemokine receptor expression on DCs. *Stem Cells 2002;20:448-459*

Correspondence: Yoichi Takaue, M.D., Hematopoietic Stem Cell Transplant Unit, National Cancer Center Hospital, 1-1 Tsukiji 5-Chome, Chuo-ku, Tokyo 104-0045, Japan. Telephone: 81-3-3542-2511; Fax: 81-3-3542-3815; e-mail: ytakaue@ncc.go.jp *Received April 25, 2002; accepted for publication June 26, 2002.* *1066-5099/2002/$5.00/0*

Introduction

Dendritic cells (DCs) are the most potent antigen-presenting cells for initiating cellular immune responses through the stimulation of naïve T cells, and their action is mainly due to the constitutive and upregulated expression of molecules related to adhesion, major histocompatibility complex (MHC), and a costimulatory pathway [1-3]. Previously, the concept of a predetermined "one cell type-one type of response," e.g., myeloid DCs induce helper T-cell type 1 (Th1) responses while lymphoid/plasmacytoid DCs induce Th2 responses, was dominant [4]. However, many investigators have since reported that DCs promote T-cell polarization depending on environmental instructions in the culture conditions or on activation signals, rather than an intrinsic ontogeny [5, 6]. DCs that generate Th1 responses may be used in clinically applicable therapeutic modalities for pathologic conditions that are caused by infections or malignant disorders, by secreting interleukin-2 (IL-2) and interferon gamma (IFN-γ) to facilitate T-cell-mediated cytotoxicity [7-9]. In contrast, DCs that generate Th2 responses may be clinically used in conditions in which Th1 responses are disturbed, e.g., transplantation, contact allergy, or autoimmune disorders, by secreting cytokines, including IL-4, IL-5, IL-6, and IL-10, to help B cells secrete protective antibodies [8, 10].

Prostaglandin E_2 (PGE_2) is produced by stromal cells and tissue-infiltrating mononuclear cells, and is an important inflammatory mediator that elevates intracellular cyclic AMP (cAMP). PGE_2 inhibits IL-2 and IFN-γ production by Th1-type cells, but not the production of IL-4 by Th2-type cells [11-13], and thereby, regulates the differentiation of naïve $CD4^+$ T cells into Th2-type $CD4^+$ T cells in vivo [11-13]. However, somewhat contradictory results have been reported regarding T-cell polarization induced by DCs that are cultured in the presence of PGE_2. *Kalinski* and coworkers [6, 14-16] reported that immature and mature DCs, generated in the presence of PGE_2, either initially or during terminal maturation, induced naïve T cells toward a Th2 response by impairing the production of IL-12. On the other hand, other investigators reported the induction of a Th1 response mediated by the greater production of IL-2 and IFN-γ with the addition of PGE_2, which resulted in higher IL-12 production [17-19]. Thus, the definitive effect of PGE_2 in the differentiation of DCs remains to be established.

Chemokines play an important role in trafficking DCs to lymphoid organs [20]. Immature DCs express various inflammatory chemokine receptors, such as CCR1, CCR4, CCR5, CCR6, and CXCR4. As maturation proceeds, DCs upregulate the constitutive expression of chemokine receptor CCR7 and downregulate inflammatory chemokine receptors, which permits DCs to be localized in lymphoid tissues where pulsed DCs stimulate effector T cells via the interaction with T-cell receptors [20-22]. In addition, previous reports have suggested that the conditions used to culture DCs affect the expression of chemokine receptors [23, 24]. Thus, this field appears to be complex, and factors that affect DC function through the expression of chemokine receptors or interaction with their ligands need to be defined.

Hence, in this study, we investigated the roles of PGE_2 in the regulation of DC function, particularly focusing on the polarization of T cells and the modification of the expression of chemokine receptors.

Materials and Methods

Medium, Reagents, and Monoclonal Antibodies

The medium used was RPMI-1640 (GIBCO-BRL; Grand Island, NY; http://www.invitrogen.com) supplemented with 10% fetal calf serum (FCS; Hyclone; Logan, UT; http://www.hyclone.com) and 1% penicillin-streptomycin (GIBCO-BRL). Recombinant human GM-CSF was provided by Kirin Brewery Company (Tokyo, Japan; http://www1.kirin.co.jp/english/r_d/pha/index.html). Recombinant IL-4, tumor necrosis factor alpha (TNF-α), and IL-2 were purchased from R&D systems (Minneapolis, MN; http://www.rndsystems.com). PGE_2 was purchased from ICN Biomedicals (Aurora, OH; http://www.icnbiomed.com) and rMIP-3β/ELC was from Dako (Kyoto, Japan; http://www.dako.dk).

Fluorescence-activated cell sorting (FACS) analysis was performed using mouse monoclonal antibodies (mAbs) against fluorescein isothiocyanate-labeled CD14 (CD14-FITC), HLA-DR-FITC, IFN-γ-FITC, phycoerythrin-labeled CD80 (CD80-PE), CD54-PE, IL-4-PE, and CD4-Percp, which were purchased from Becton Dickinson (San Jose, CA; http://www.bd.com). CD40-FITC and CD86-FITC antibodies were from PharMingen (San Diego, CA; http://www.bdbiosciences.com/pharmingen), and mAbs against CD45RA-FITC, CD1a-PE, CD45RO-PE, and CD83-PE were from Coulter-Immunotech (Miami, FL; http://www.coulter.com). Biotinylated mAbs against CCR1, CXCR4, and CCR6 were purchased from Dako. Isotype controls were run in parallel. Cell debris was eliminated from the analysis by forward and side scatter gating. The samples were acquired on a FACS Caliber cell sorter (Becton Dickinson) and analyzed with CellQuest software (Becton Dickinson).

Generation of Immature DCs and Induction of Mature DCs

$CD14^+$ cells isolated from leftover peripheral blood stem cell (PBSC) products, which were collected from healthy donors mobilized with G-CSF for allogeneic trans-

plantation after obtaining a consent form, were used to generate DCs. In brief, the PBSC products produced 2-6 × 10^8 cells after washing the material remaining in the apheresis bags. $CD14^+$ cells were isolated from the PBSC products (>85% purity) using the magnetic activated cell sorter (MACS) according to the manufacturer's instructions (Miltenyi Biotec; Auburn, CA; http://www.miltenyi biotec.com). To generate immature DCs, the $CD14^+$ cells were cultured at a density of 1 × 10^6 cells per 1 ml of culture medium with one of the following combinations of cytokines: A) GM-CSF (50 ng/ml) and IL-4 (50 ng/ml) or B) GM-CSF (50 ng/ml), IL-4 (50 ng/ml), and PGE_2 (10^{-7} M). Freshly prepared cytokines were added every other day. Maturation of DCs was induced by adding TNF-α (50 ng/ml) with or without PGE_2 (10^{-7} M) to each group of cultures on day 6. DCs were harvested as immature (day 6) or mature (day 9) cells for morphologic, phenotypic, or functional evaluations. Additionally, the culture supernatants were collected on the same days and frozen at –20°C until measurement of IL-10 and IL-12 levels using enzyme-linked immunosorbent assays (ELISA).

Immature or mature DCs (3 × 10^4 cells) were then prepared on cytospin slides with centrifugation at 400 revolutions per minute (rpm) for 5 minutes. These slides were dried, fixed with Carnoy's solution (ethanol:acetic acid:chloroform = 6:1:3), stained with May-Grunwald-Giemsa stain, and visualized by light microscopy.

T-Cell Preparation

$CD3^+$ cells for the mixed lymphocyte reaction (MLR) assay were obtained from the peripheral blood of a healthy donor using human T-cell enrichment columns (R&D Systems). Naive $CD4^+CD45RA^+$ T cells for the cytokine assay were isolated from the PBSC products by two-step positive selection using MACS. $CD8^+$ cells for the cytotoxic assay were also isolated from autologous PBSC products by positive selection using MACS. The purity of isolated cells was >90% for $CD3^+$ cells and >95% for naïve $CD4^+CD45RA^+$ T cells or $CD8^+$ cells.

Endocytic Activity

Cells (1 × 10^5), suspended in 100 μl of culture medium, were incubated with FITC-dextran (20 μg/ml) for 1 hour at 37°C in a water bath or at 4°C on ice, and then washed thoroughly with cold buffer consisting of phosphate-buffered saline (PBS), 5 mM EDTA, and 2% FCS. The samples were acquired on a FACS Caliber cell sorter, with 10^4 gating events for each sample, and analyzed with CellQuest software. The results were expressed as a mean fluorescence intensity (MFI) index calculated as the ratio of the MFI of the sample to the MFI of an isotype-matched control.

Allogeneic MLR

Allogeneic $CD3^+$ cells (5 × 10^4/well), obtained from healthy donor blood, were cocultured in 96-well, round-bottomed culture plates with graded doses (2 × 10^2 – 5 × 10^4) of irradiated (30 Gy) DCs that were harvested from each group on day 6 or 9 of culture. After 5 days, the cells were pulsed with 1 Ci [^{3}H]-methylthymidine per well for 16 hours, harvested, and analyzed in a liquid scintillation counter. The results were expressed as the mean counts per minute (cpm) ± the standard error (SE) of results obtained with four different samples, each performed in triplicate.

Intracellular Cytokine Staining

DCs (1.05 × 10^5 cells/500 μl) that were harvested on day 6 or 9 were primed with 50 ng/ml staphylococcal exotoxins (Toxin Technology Inc.; Sarasota, FL; http://www.toxintechnology.com), which contain an enterotoxin (SEA-SEE), exfoliative toxins (ETA and ETB), and toxic shock syndrome toxin (TSST-1), for 1 hour at 37°C and then irradiated (30 Gy). DCs were cocultured with naïve $CD4^+CD45RA^+$ T cells (5 × 10^5/well) in the culture medium at ratios of 1:5 (total volume of 600 μl) and 1:300 (total volume of 500 μl) in 24-well plates. On day 5, the cells were washed out completely and expanded with fresh medium containing 500 U/ml of IL-2. Two hundred fifty microliters of culture supernatant were then replaced with medium of the same concentration every 3 days. On day 14, the supernatant was collected and frozen at –20°C until ELISA assays for IFN-γ and IL-4 were performed. The intracellular cytokine concentrations of the harvested T cells were measured by FACS analysis, as described previously. Briefly, T cells (10^6) were stimulated with phorbol myristate acetate (PMA) (10 ng/ml) and ionomycin (1 μg/ml) for 4 hours in a 37°C water bath. Brefeldin A (10 μg/ml) was added during the last 2 hours of incubation to prevent cytokine secretion. Cells were collected, fixed with 1% paraformaldehyde (Becton Dickinson), permeabilized with a commercial solution (Becton Dickinson), and stained with FITC-labeled anti-IFN-γ (IgG2a) and PE-labeled anti-IL-4 (IgG1) mAbs. The samples were processed by a FACS Caliber cell sorter, with at least 10^4 gating events for each sample, and analyzed with CellQuest software.

Cytotoxic T-Lymphocyte (CTL) Assay

Mature DCs (5 × 10^5) cultured from $HLA\text{-}A24^+$ donors were loaded with 10 μM Epstein-Barr virus (EBV)-derived peptide (TYGPVFMCL), which can bind to HLA-A2402 as reported by *Lee et al.* [25], for 2 hours at 37°C. In 24-well plates, autologous $CD8^+$ T cells were cocultured as effector cells at a ratio of 2:1 with DCs in 2 ml of medium (RPMI 1640:AIM-V = 1:1) containing 10% FCS (Sigma; St. Louis, MO; http://www.sigmaaldrich.com), 1% penicillin-strepto-

mycin (GIBCO-BRL), and 0.1 mM/l nonessential amino acids supplemented with 100 U/ml IL-2 for 10 days; half the medium was changed every 3 days. BEC-2 cell lines (HLA-A2402) and Bamb-2 cell lines (HLA-A1/A26) generated by EBV-transformed B-lymphoblastoid cell line from an EBV^+ healthy donor were kindly provided by *Dr. Itoh* (Kurume University School of Medicine; Kurume, Japan). The BEC-2 cells and Bamb-2 cells, as target cells, were loaded at a concentration of 1×10^6 cells/ml with 10 μM EBV peptide and incubated for 2 hours at 37°C in 5% CO_2. Effector cells were cocultured with target cells at effector-to-target ratios of 2:1, 5:1, and 10:1 in 96-well round-bottomed culture plates (total volume of 200 μl) in duplicate or triplicate. After overnight incubation at 37°C in 5% CO_2, the human IFN-γ concentration of the supernatant was measured (pg/ml) using ELISA according to the manufacturer's instructions (OptEIA™ Human IFN-γ Set; PharMingen).

Cytokine Assay by ELISA

IL-10 (limit of sensitivity, 3.9 pg/ml) and IL-12 (limit of sensitivity, 0.5 pg/ml) were measured in the supernatant collected at day 6 or 9 of DC culture using Quantikine Immunoassay Kits (R&D Systems) according to the manufacturer's instructions. IL-4 (limit of sensitivity, 0.13 pg/ml) and IFN-γ were measured in the supernatant of naïve $CD4^+CD45RA^+$ cells obtained at day 14. Cytokines were quantified using a microplate reader at 450-490 nM, plotted against a standard curve with the cytokines, and expressed in pg/ml.

Transmigration Assay

To evaluate the chemotactic effects of DCs stimulated with chemokines, a double-chamber system was used, with previously described modifications [26]. Briefly, polycarbonate membranes with 8-μm pore size filters (Chemotaxicell™; Kurabo; Osaka, Japan; http://www.kurabo.co.jp) were placed on 24-well culture plates to separate the upper and lower chambers. Macrophage inflammatory protein (MIP)-3β for mature DCs was seeded at concentrations of 1, 10, and 100 nM diluted with 500 μl of culture medium in the lower chambers. Next, $0.5\text{-}1 \times 10^5/100$ μl mature DCs were added to the upper chambers. After overnight incubation at 37°C in 5% CO_2, the cells that migrated into the lower chambers were collected. Using a Coulter counter, only cells larger than 12 μm were counted, to eliminate lymphocyte contamination. The results were expressed as a net migration percentage calculated as: (number of cells that migrated into the lower chamber containing chemokines—number of cells that migrated in medium alone)/total number of cells loaded in the upper chamber × 100.

Calcium Flux Measurement

Mature DCs, at a concentration of 1×10^6 cells/ml, were loaded with 5 μg/ml Fluo-3AM (Calbiochem; San Diego, CA), incubated for 30 minutes in a 37°C water bath, and centrifuged for 10 minutes at 1,500 rpm. The DCs were then resuspended in RPMI with 5% FCS at 1×10^6 cells/ml. Calcium flux was measured at 450 nM as a function of time in response to 100 nM MIP-3β for mature DCs, with 3 mM EGTA and as a negative control and ionomycin (10 ng/ml) as a positive control, using a FACS Caliber cell sorter, and analyzed using FlowJo software (Becton Dickinson).

Reverse Transcription-Polymerase Chain Reaction (RT-PCR) for CCR7

Total RNA was extracted from $1\text{-}2 \times 10^6$ mature DCs using an RNeasy Mini Kit (Qiagen; Hilden, Germany; http://www.qiagen.com). The cDNA synthesized from total RNA by Moloney murine leukemia virus reverse transcriptase (Stratagene; Austin, TX; http://www.stratagene.com) was subjected to RT-PCR using 30 cycles at 94°C for 0.5 minutes, 57.5°C for 1 minute, and 72°C for 1 minute for CCR7 (TaKaRa; Tokyo, Japan; http://www.takara bio.co.jp/english/index.htm). The sense and anti-sense oligonucleotide primers for CCR7 were 5′-CGCGTC-CTTCTCATCAGCAA-3′ and 5′-GTCCCGACAGGAA-GACCACT-3′, respectively. PCR products were identified by electrophoresis on 2% agarose gels that were photographed.

Statistical Analysis

Values are presented as the mean ± SE. The Mann-Whitney *U* test was used to compare values between subgroups using SPSS 10.0 software. p values <0.05 were considered statistically significant.

Results

Morphology, Phenotypic Features, and Endocytic Activity

With May-Grünwald-Giemsa staining; cells cultured with or without PGE_2 for 6 or 9 days showed similar typical features of immature DCs (large cells with an irregular outline and a few veils) or mature DCs (large, veiled, nonadherent appearance and highly motile). However, when the cultured cells on the plates were directly observed without staining under phase-contrast microscopy on day 9, the cells cultured in the presence of PGE_2 had less branching and fewer veiled structures than those without PGE_2 (data not shown).

With FACS analysis, the expression of CD1a, CD40, and CD83 in immature DCs treated with PGE_2 was significantly lower than that in control cells without PGE_2 (means 8%, 40%, and 2% versus 73%, 86%, and 11%, respectively;

Table 1. Comparison of phenotypes of immature DCs (iDC) cultured with GM-CSF + IL-4 and immature DCs (PGE_2-iDC) cultured in the presence of PGE_2 on day 6

	iDC	PGE_2-iDC	*p* value
CD14	12.3 ± 3.5	85.4 ± 3.4	0.001
CD1a	72.9 ± 6.8	8.1 ± 1.9	0.001
HLA-DR	98.9 ± 0.6	98.9 ± 0.5	0.953
CD80	57.2 ± 8.4	40.6 ± 14.3	0.298
CD83	11.3 ± 3.2	2.3 ± 0.8	0.028
CD86	52.7 ± 6.2	69.8 ± 6.6	0.105
CD40	86.4 ± 6.7	40.0 ± 9.0	0.004
CD54	99.0 ± 0.2	97.3 ± 1.5	0.245

Values are percentages ± SE.

$p = 0.001$, $p = 0.004$, and $p = 0.028$, respectively) as shown in Table 1. The expression of CD14 on immature DCs was retained in cells cultured with PGE_2, while this was lost in control cells (mean 86% versus 12%, $p = 0.001$, Table 1). Other phenotypes, including HLA-DR, CD80, CD86, and CD54 were similarly highly expressed on both cells, regardless of the presence of PGE_2.

When mature DCs, which were treated with TNF-α alone as a maturating agent, were evaluated by FACS, the cells with added PGE_2 showed a significantly lower expression of CD1a than control cells (88% versus 65%, $p = 0.024$, Table 2). TNF-α also induced a similar maturation pattern in immature DCs that were initially cultured with PGE_2. CD1a expression in these cells was almost completely recovered when PGE_2 was removed compared with the continuous presence of PGE_2 (78% versus 19%, $p = 0.004$, Table 2). However, the DCs from which PGE_2 had been removed showed a lower expression of CD83 and CD86, compared with those in the continuous presence of PGE_2 (means of 62% and 72% versus 88% and 92%, respectively, $p = 0.016$ and $p = 0.01$, Table 2).

We then used FITC-dextran to measure mannose receptor-mediated endocytosis in immature and mature DCs induced by various cytokine combinations. In immature DCs, the MFI index tended to be higher in the presence of PGE_2 than in the controls (29 ± 11 versus 16 ± 6). However, the ability to take up soluble antigen decreased as DCs matured (data not shown).

DC with Added PGE_2 Showed a High MLR at a High DC/T-Cell Ratio

Immature DCs cultured with PGE_2 had a higher capacity to stimulate allogeneic $CD3^+$ T cells than control cells at a higher DC/T-cell ratio ($p = 0.003$ and $p = 0.007$ at ratios of 1:1 and 1:2, respectively, Fig. 1A). On the other hand, there were lower allostimulatory effects in the MLR at a lower cell ratio, although variations were noted among different samples ($p < 0.001$ and $p = 0.0013$ at ratios of 1:16 and 1:128, respectively, Fig. 1A). These findings suggest that PGE_2 affected the allostimulatory capacity of DCs depending upon the DC/T-cell ratio. The allostimulatory capacity of mature DCs on $CD3^+$ T cells was also higher when the cells were cultured with PGE_2 than without PGE_2 at a high cell-dose ratio (Fig. 1B).

Effects of PGE_2 on DC-Mediated Th1 Polarization of Naive T Cells

When immature DCs, which had been cultured in the presence of PGE_2, were used to induce the differentiation of naïve T cells, there was a shift toward Th1 polarization, as judged by elevated IFN-γ levels, minimal expression of IL-4 by intracellular cytokine staining, and ELISA assays, although a slightly lower excretion of IFN-γ than in controls was observed in the presence of PGE_2 at high DC/T-cell ratios (1:5). Mature DCs also showed a higher level of IFN-γ and a lower level of IL-4, but there was no difference in cytokine levels between different culture conditions

Table 2. Comparison of phenotypes of mature DCs cultured with various cytokine combinations on day 9

	iDC + TNF-α	iDC + TNF-α + PGE_2	PGE_2-iDC + TNF-α	PGE_2-iDC + TNF-α + PGE_2
CD14	0.6 ± 0.2	1.0 ± 0.2	5.0 ± 0.9	5.7 ± 1.4
CD1a	87.9 ± 2.6	65.1 ± 8.4	77.8 ± 6.5	18.9 ± 5.4
HLA-DR	99.8 ± 0.0	99.7 ± 0.1	99.7 ± 0.1	99.5 ± 0.2
CD80	95.4 ± 2.7	96.3 ± 1.7	94.9 ± 3.1	96.1 ± 1.6
CD83	85.9 ± 2.4	90.0 ± 3.1	61.8 ± 7.4	87.9 ± 3.7
CD86	93.6 ± 1.6	97.5 ± 0.6	72.1 ± 6.3	92.3 ± 3.9
CD40	99.4 ± 0.3	96.8 ± 1.4	99.6 ± 0.3	99.2 ± 0.4
CD54	98.5 ± 0.7	95.2 ± 1.9	99.7 ± 0.1	99.4 ± 0.3

Values are percentages ± SE.

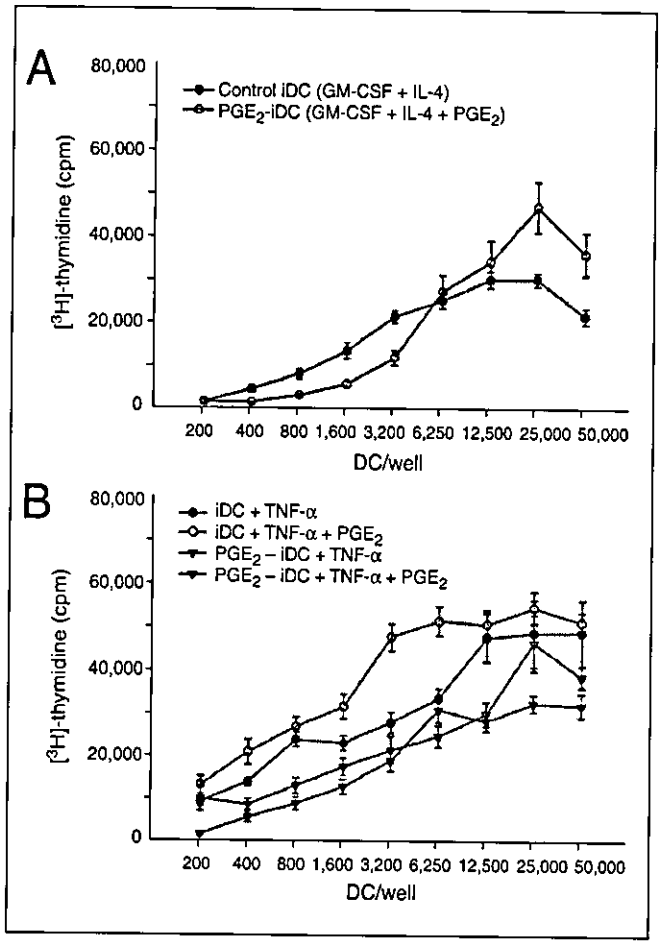

Figure 1. Allogeneic T-cell stimulatory capacity of immature DCs (A) and mature DCs (B) cultured with or without PGE_2. *$CD3^+$ cells (5×10^4 cells/well) isolated from healthy donors were cocultured with graded doses of irradiated DCs, and on day 5, [^{3}H]-methylthymidine was added 16 hours before measurement of the proliferative response. Data shown are the mean cpm (± SE) of triplicate cultures from four independent experiments.*

(Figs. 2 and 3). The addition of PGE_2 resulted in a lower IFN-γ production by naïve T cells, and removal of PGE_2 at maturation induced a complete recovery of IFN-γ secretion (Fig. 3). This suggests that, in the presence of PGE_2, immature or mature DCs induce naïve T cells to differentiate toward a Th1 response and that PGE_2 inhibits the Th1 polarization of naïve T cells. Additionally, T cells cocultured with immature or mature DCs at a low cell ratio (1:300) showed a greater production of IL-4 and a lower production of IFN-γ than those at a high cell ratio, regardless of the

Figure 2. Immature (A) and mature DCs (B) cultured in the presence of PGE_2 induced the differentiation of naïve $CD4^+CD45RA^+$ cells to a Th1 response at a high ratio of DCs/T cells (1:5) and to a Th1/Th2 response at a low ratio (1:300). *Naïve T cells were cocultured with DCs after being pulsed with staphylococcal exotoxins, expanded with the addition of 500 U/ml IL-2 from day 5, and harvested on day 14. Intracellular cytokine (IFN-γ and IL-4) concentrations were measured after restimulation with PMA and ionomycin for 4 hours on day 14. The data shown are from one representative experiment. Similar data were obtained in two other subgroups of mature DCs.*

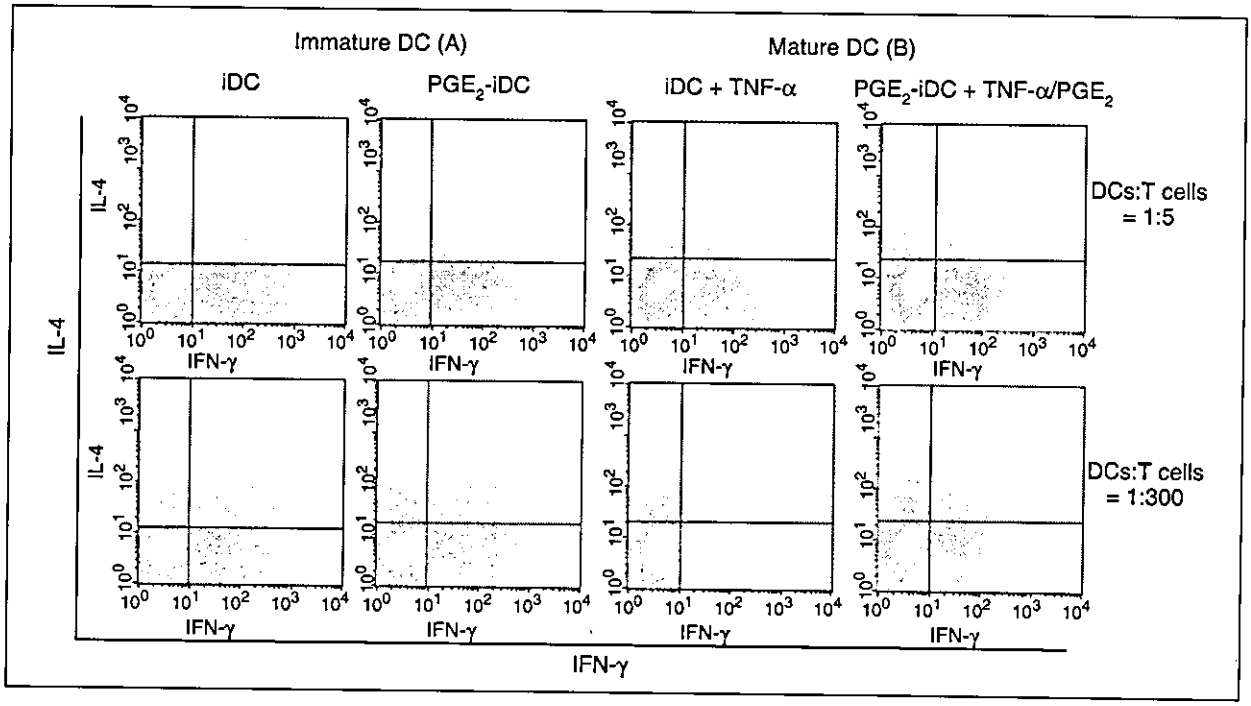

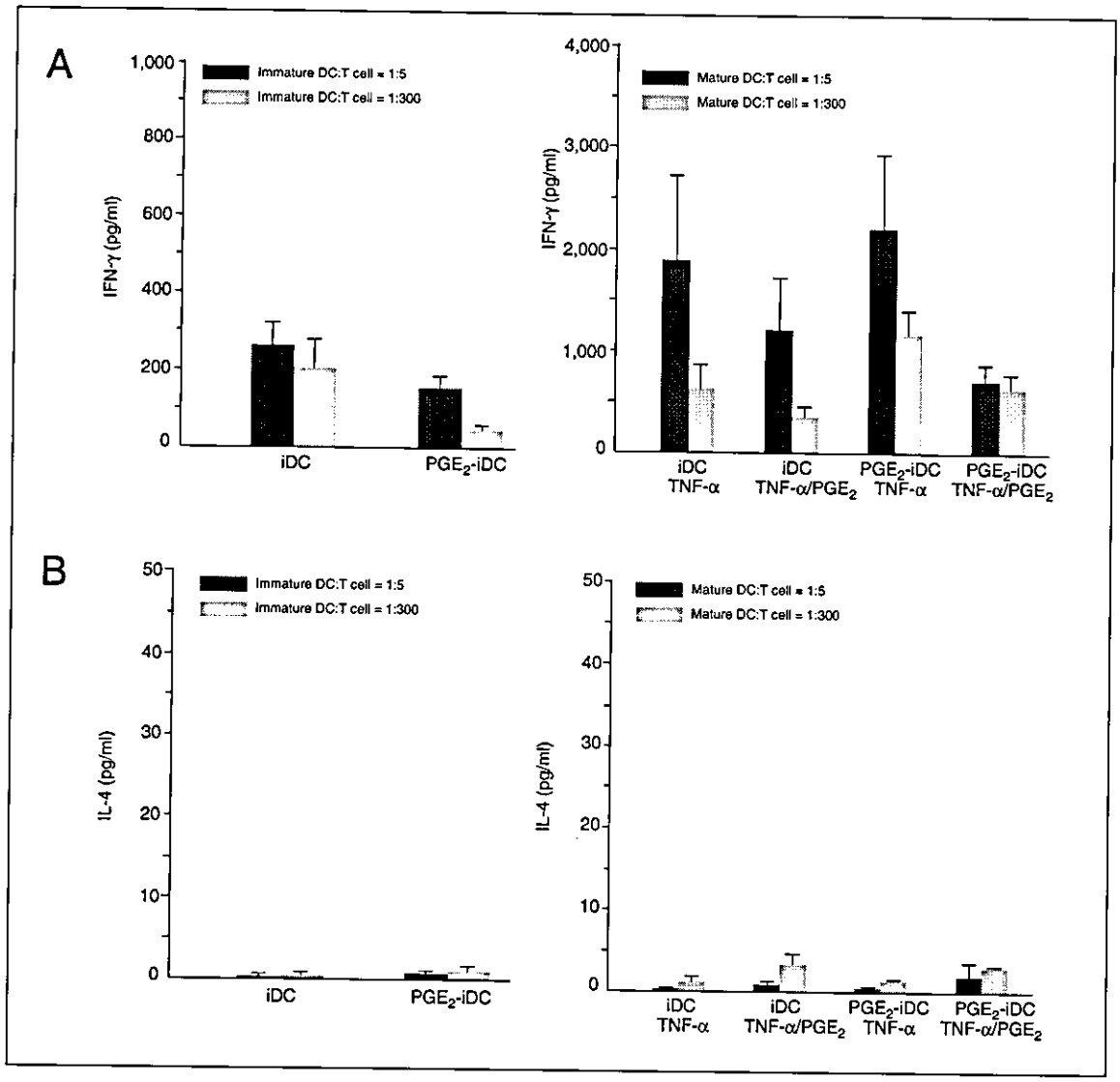

Figure 3. Measurement of IFN-γ (A) and IL-4 (B) by ELISA in supernatant (on day 14) of naïve CD4⁺CD45RA⁺ T cells stimulated by immature or mature DCs. *DCs under culture with PGE_2 induced naïve T cells to secrete high amounts of IFN-γ, although less than that secreted by control cells, but a low amount of IL-4 at a high ratio of DCs/T cells (1:5). However, naïve T cells at a low ratio (1:300) tended to have a lower IFN-γ level and a greater IL-4 level than those at a high ratio (1:5). Data shown are the mean ± SE from four independent experiments.*

presence of PGE_2. This finding suggests that naïve T cells are polarized toward both Th1 and Th2 responses at a low DC/T-cell ratio (Figs. 2 and 3).

Levels of IL-12 and IL-10 measured in the culture supernatant of immature or mature DCs were basically very low, with no difference between the presence or absence of PGE_2 (Fig. 4). In this study, IL-12 and IL-10 were measured in the basal state without any other stimulation. Therefore, this finding suggests that T-cell polarization by DCs in the basal state does not depend on IL-10 or IL-12.

Mature DCs Cultured with PGE_2 Did not Augment the Cytotoxicity of CD8⁺ T Cells Against BEC-2 Target Cells

We compared the CTL responses of autologous CD8⁺ T cells supported by mature DCs cultured with or without PGE_2, after the observation that DCs in the presence of PGE_2 induced naïve T-cell differentiation into a Th1 response. CD8⁺ T cells that were stimulated with EBV-pulsed mature DCs showed stronger CTL responses against BEC-2 target cells, as measured by IFN-γ ELISA assay, than against Bamb-2 target cells. This stimulation depended on the effector-to-target ratio. However, the

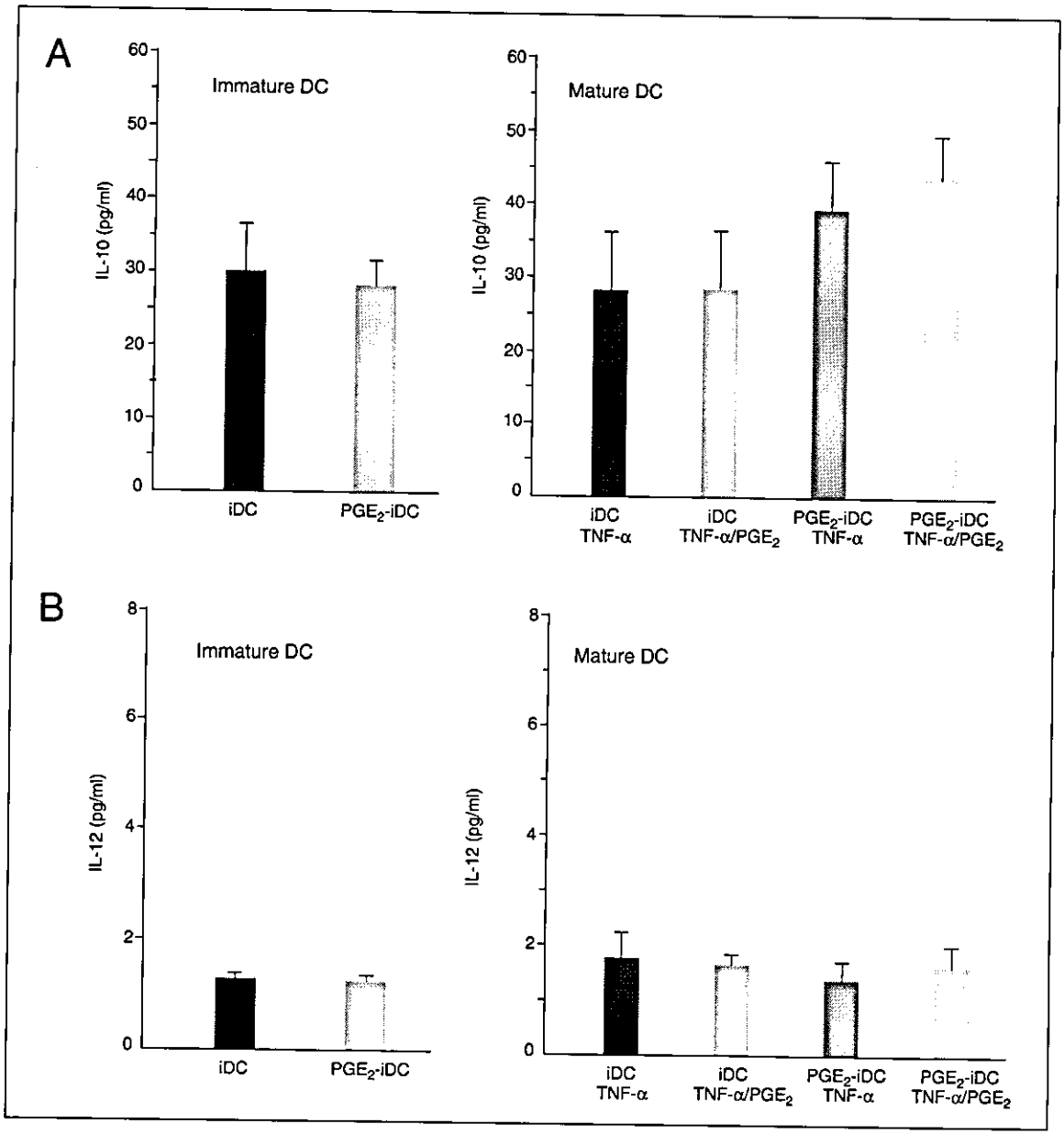

Figure 4. Measurement of IL-10 (A) and IL-12 (B) in supernatant of immature or mature DC culture without further stimulation. DCs, regardless of the presence or absence of PGE_2, secreted very low levels of both cytokines in the basal state, suggesting that such secretion is not related to IFN-γ secretion. The results represent the mean (pg/ml) ± SE of at least seven independent experiments.

potency of CTL itself was not augmented in the presence of PGE_2 (Fig. 5).

PGE_2 Did not Affect the Expression of Chemokine Receptors by Immature or Mature DCs

To evaluate whether the expression of chemokine receptors on DCs was affected by PGE_2, we performed a FACS analysis using mAbs to chemokine receptors in immature DCs, a transmigration test and calcium flux measurement using chemokines in mature DCs, and RT-PCR of CCR7 in mature DCs.

Phenotypic analysis of immature DCs using flow cytometry showed a high expression of CCR1 and CXCR4, with no difference between cell cultures with and without PGE_2, whereas CCR6 was not expressed at all in immature DCs (Fig. 6). In mature DCs, there was a high migration and a high calcium flux in response to MIP-3β, the ligand for CCR7, regardless of whether DCs were treated with

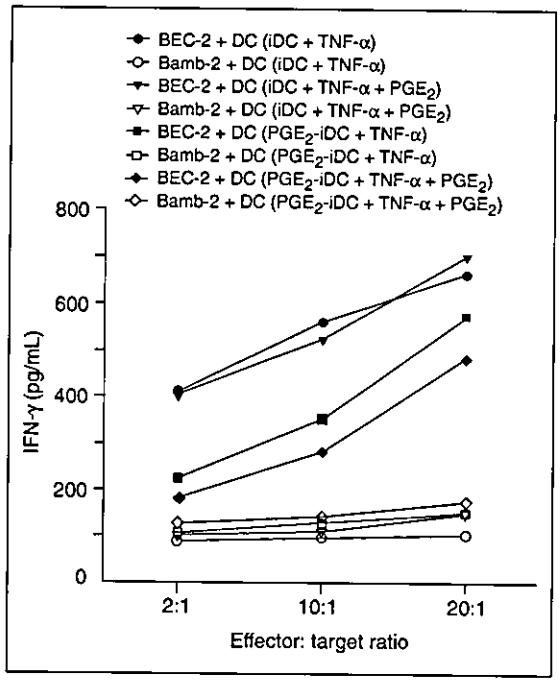

Figure 5. Autologous CD8⁺ T cells cocultured with mature DCs showed higher cytolytic activity against BEC-2 target cells at a high effector-to-target ratio than against Bamb-2 target cells. *However, the addition of PGE_2 did not affect the production of T cell IFN-γ by mature DCs. Autologous CD8⁺ T cells were cocultured with mature DCs pulsed with EBV-derived peptide, expanded with 100 U/ml IL-2, and, on day 8, restimulated with BEC-2 or Bamb-2 target cells at various effector-to-target ratios. After overnight culture, the IFN-γ concentration in the supernatant was measured by ELISA assay. The data are from one representative experiment.*

PGE_2 or not (Fig. 7). Additionally, RT-PCR to examine the expression of CCR7 showed similar positive reactions in mature DCs cultured with or without PGE_2 (Fig. 7).

Discussion

This study showed that, in the presence of PGE_2, DCs enhanced naïve T cells to polarize toward a Th1 response, independent of IL-12 secretion in the basal state, without any change in the expression of chemokine receptors on DCs. Moreover, PGE_2 induced a lower expression of CD1a and a persistently higher expression of CD14 in immature DCs, which is consistent with previous reports by other groups [14, 16, 17, 19]. Additionally, the observed phenotypic findings were similar to those for monocyte-derived macrophages cultured with M-CSF [27]. While monocyte-derived macrophages had little allostimulatory capacity, immature DCs derived from CD14⁺ cells with PGE_2 elicited a stronger MLR response than that of control cells cultured without PGE_2 [3, 28]. The reported allostimulatory capacity of T cells has varied when DCs were cultured in the presence of PGE_2 [15, 17, 18, 28].

This confusion is likely the result of different culture conditions, i.e., various cytokine combinations and culture

Figure 6. FACS analysis of chemokine receptor expression in immature DCs. *Immature DCs showed a high expression of CCR1 and CXCR4 (solid line), but no expression of CCR6 (solid line). However, the addition of PGE_2 did not affect the expression of these chemokine receptors on CD14⁺-cell-derived DCs. Dotted lines represent isotype-matched negative controls.*

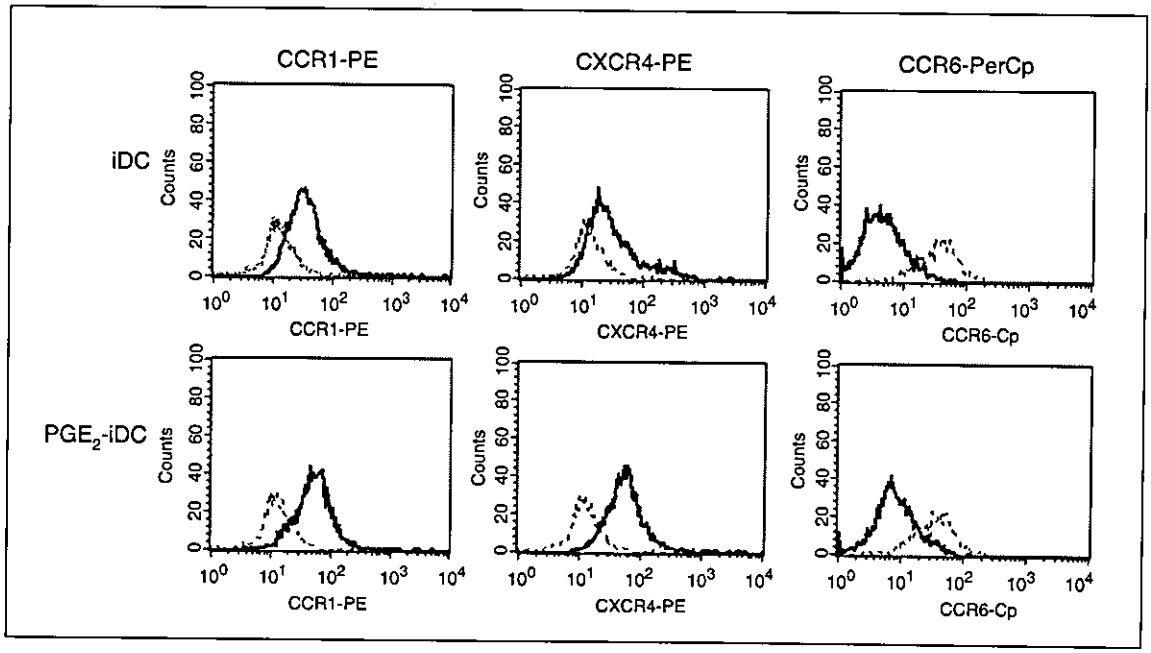

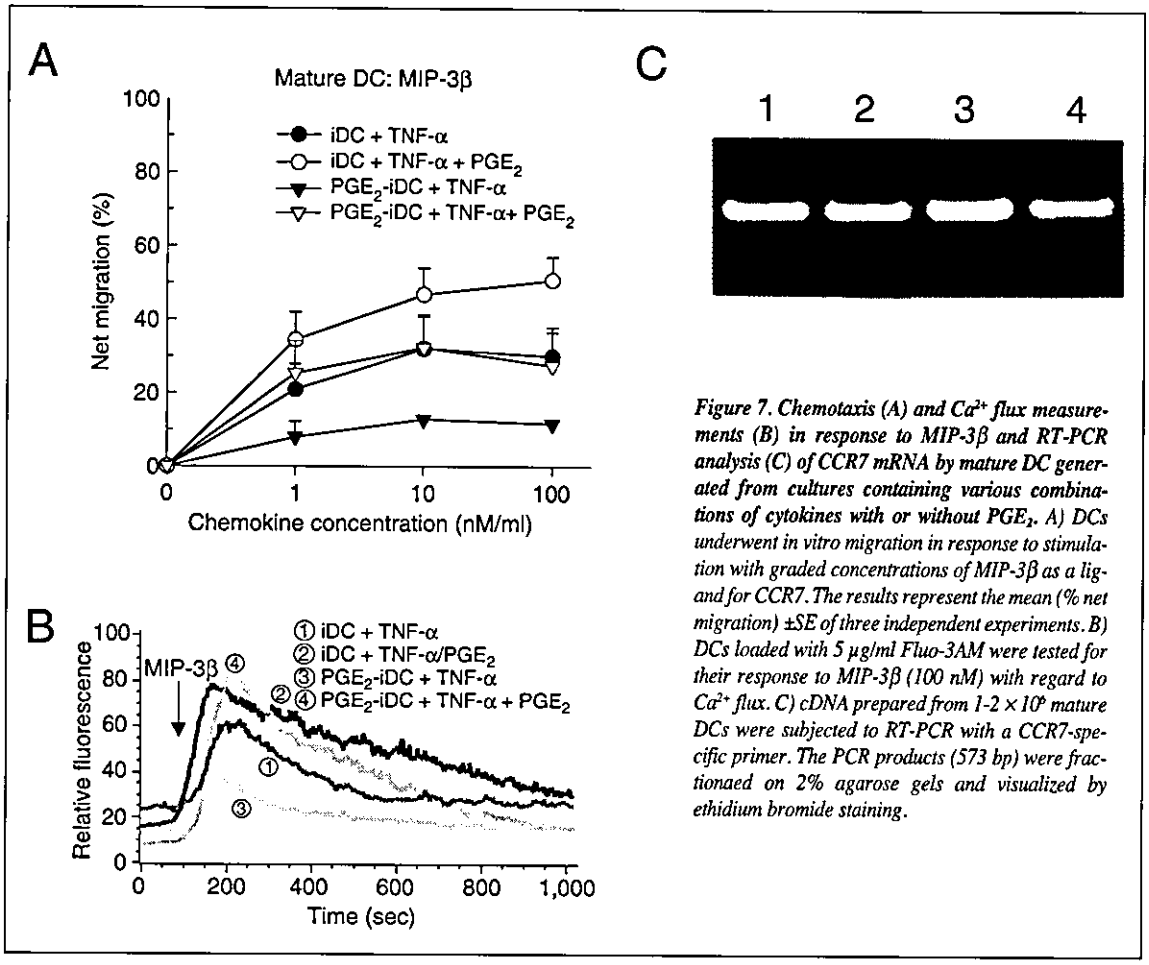

Figure 7. Chemotaxis (A) and Ca^{2+} flux measurements (B) in response to MIP-3β and RT-PCR analysis (C) of CCR7 mRNA by mature DC generated from cultures containing various combinations of cytokines with or without PGE_2. A) DCs underwent in vitro migration in response to stimulation with graded concentrations of MIP-3β as a ligand for CCR7. The results represent the mean (% net migration) ±SE of three independent experiments. B) DCs loaded with 5 µg/ml Fluo-3AM were tested for their response to MIP-3β (100 nM) with regard to Ca^{2+} flux. C) cDNA prepared from 1-2 × 10^6 mature DCs were subjected to RT-PCR with a CCR7-specific primer. The PCR products (573 bp) were fractionaed on 2% agarose gels and visualized by ethidium bromide staining.

media. Without the standardization of culture conditions, the results cannot be directly compared. In this study, immature DCs cultured in the presence of PGE_2 showed variable allostimulatory capacity that totally depended on the ratio of DC to T cells; a higher MLR response was seen at a higher ratio and a lower MLR response was seen at a lower ratio. In this study, DCs cultured with added PGE_2 during maturation had an enhanced allostimulatory capacity for $CD3^+$ T cells compared with controls without PGE_2.

Skewing of naïve T cells toward a Th1 or Th2 response is a crucial process in determining the ultimate outcome of the immune response, and this is affected by the culture environment of antigen-presenting DCs, as well as by the modulation of T-cell-receptor-mediated activation signals [29-31]. In this study, PGE_2 caused DCs to induce naïve T cells, which secreted IFN-γ independent of IL-12 secretion in the basal state, with a Th1 response. Hence, some of our findings are consistent with recently published reports that PGE_2 promoted a Th1 response [17, 19]. However, the results from these reports suggested that IL-12 production by DCs was crucial for increasing the production of IL-2 and IFN-γ [17-19]. This discrepancy regarding IL-12 production between our study and others might be explained by differences in the supernatant sample used for the measurement; we measured the supernatant of DCs cultured in the presence of PGE_2 without further stimulation, while others used supernatant after stimulating cells with various agents or supernatant of stimulated naïve T cells. A recent report supports our observation by finding only slight IL-12 secretion measured in samples in the basal state without further stimulation [32]. In addition, there is an interesting report that a high DC/T-cell ratio (1:4) resulted in a mixed Th1/Th2 response, while a low DC/T-cell ratio (1:300) induced T cells to become Th2 effectors, suggesting that the polarization of naïve T cells was influenced by their environment [33]. We showed that $CD14^+$-cell-derived DCs induced naïve T-cell differentiation with a Th1/Th2 response at a lower DC/T-cell ratio (1:300), although we used different DC maturation agents and a different stimulation of T cells by DCs than the previous report [33].

In contrast, *Kalinski* and coworkers [6, 14-16] reported that PGE_2 induced type 2-polarized DCs, which promote

the development of Th2 cells from naïve T cells via the inhibition of IL-12 production by DCs. Although *Steinbrink et al.* [19] argued that differences in the medium and cytokine combinations used for DC culture or a different ratio of T cells to DCs at stimulation produced contradictory results, we think that this discrepancy mainly resulted from the stimulating agents, such as cytokines or superantigen, used to produce DC maturation or to augment naïve T-cell stimulation, since we used a similar medium and ratio of T cells to DCs to those of *Kalinski* and coworkers. In that study, however, PGE_2 inhibited Th1 polarization of naïve T cells by DCs in the basal state compared with controls. Based on this observation, it is still possible that the induction of a Th2 response of naïve T cells by DCs is promoted by strong stimulating agents.

We evaluated the CTL response to examine the possible clinical application of our culture system, since DCs in the presence of PGE_2 induced a significant Th1 response. Unfortunately, the DCs cultured with PGE_2 did not produce a stronger CTL response than control cells cultured without PGE_2, thus excluding the possibility of clinical application. On the other hand, much attention has recently been focused on chemokine receptors as promising targets for clinical application. When immature DCs undergo maturation with various agents, CCR7, a constitutive chemokine receptor, is upregulated, and inflammatory chemokine receptors are downregulated, allowing the migration of DCs to lymphoid tissues [20-22]. In general, CCR6, a specific receptor for MIP-3β/liver and activation-regulated chemokine, is highly expressed in immature DCs derived from $CD34^+$ cord blood precursors, but not in $CD14^+$ peripheral blood monocyte-derived DCs [20-22]. Recently, *Yang et al.* [24] reported that CCR6 was also expressed in monocyte-derived DCs cultured in the presence of transforming growth factor-1 and that this contributed to the regulation of the trafficking of DCs, suggesting that DC culture conditions significantly affect the expression of chemokine receptors. In our study, immature DCs cultured in the presence of PGE_2 showed a high expression of CCR1 and CXCR4, but did not express CCR6 by a phenotype analysis. In addition, there was no difference in the expressions of CCR7 between mature DCs cultured with and without PGE_2, which supports the notion that PGE_2 does not directly influence the expression of chemokines.

In conclusion, our findings suggest that DCs cultured in the presence of PGE_2 enhance the differentiation of naïve T cells toward the Th1 type, independent of IL-12 secretion in the basal state, and that PGE_2 does not have any significant effect on chemokine receptor expression by DCs.

ACKNOWLEDGMENTS

This research was supported by a Grant-in-Aid for Scientific Research from the Ministry of Health, Labor and Welfare of Japan. We thank *Dr. Kyogo Itoh* of the Kurume University School of Medicine, Kurume, Japan, for kindly providing the BEC-2 and Bamb-2 cell lines.

REFERENCES

1 Steinman RM. The dendritic cell system and its role in immunogenicity. Annu Rev Immunol 1991;9:271-296.

2 Hart DN. Dendritic cells: unique leukocyte populations which control the primary immune response. Blood 1997;90:3245-3287.

3 Avigan D. Dendritic cells: development, function and potential use for cancer immunotherapy. Blood Rev 1999;13:51-64.

4 Grabbe S, Kampgen E, Schuler G. Dendritic cells: multi-lineal and multi-functional. Immunol Today 2000;21:431-433.

5 Rissoan MC, Soumelis V, Kadowaki N et al. Reciprocal control of T helper cell and dendritic cell differentiation. Science 1999;283:1183-1186.

6 Vieira PL, de Jong EC, Wierenga EA et al. Development of Th1-inducing capacity in myeloid dendritic cells requires environmental instruction. J Immunol 2000;164:4507-4512.

7 Trinchieri G, Scott P. The role of interleukin 12 in the immune response, disease and therapy. Immunol Today 1994;15:460-463.

8 Banchereau J, Steinman RM. Dendritic cells and the control of immunity. Nature 1998;392:245-252.

9 Tarte K, Klein B. Dendritic cell-based vaccine: a promising approach for cancer immunotherapy. Leukemia 1999;13:653-663.

10 O'Garra A, Murphy K. T-cell subsets in autoimmunity. Curr Opin Immunol 1993;5:880-886.

11 Davies P, Bailey PJ, Goldenberg MM et al. The role of arachidonic acid oxygenation products in pain and inflammation. Annu Rev Immunol 1984;2:335-357.

12 Betz M, Fox BS. Prostaglandin E_2 inhibits production of Th1 lymphokines but not of Th2 lymphokines. J Immunol 1991;146:108-113.

13 Snijdewint FG, Kalinski P, Wierenga EA et al. Prostaglandin E_2 differentially modulates cytokine secretion profiles of human T helper lymphocytes. J Immunol 1993;150:5321-5329.

14 Kalinski P, Hilkens CM, Snijders A et al. Dendritic cells, obtained from peripheral blood precursors in the presence of PGE_2, promote Th2 responses. Adv Exp Med Biol 1997;417:363-367.

15 Kalinski P, Hilkens CM, Snijders A et al. IL-12-deficient dendritic cells, generated in the presence of prostaglandin E_2,

promote type 2 cytokine production in maturing human naïve T helper cells. J Immunol 1997;159:28-35.

16 Kalinski P, Schuitemaker JH, Hilkens CM et al. Prostaglandin E_2 induces the final maturation of IL-12-deficient $CD1a^+CD83^+$ dendritic cells: the levels of IL-12 are determined during the final dendritic cell maturation and are resistant to further modulation. J Immunol 1998;161:2804-2809.

17 Rieser C, Bock G, Klocker H et al. Prostaglandin E_2 and tumor necrosis factor alpha cooperate to activate human dendritic cells: synergistic activation of interleukin 12 production. J Exp Med 1997;186:1603-1608.

18 Rieser C, Papesh C, Herold M et al. Differential deactivation of human dendritic cells by endotoxin desensitization: role of tumor necrosis factor-alpha and prostaglandin E_2. Blood 1998;91:3112-3117.

19 Steinbrink K, Paragnik L, Jonuleit H et al. Induction of dendritic cell maturation and modulation of dendritic cell-induced immune responses by prostaglandins. Arch Dermatol Res 2000;292:437-445.

20 Cyster JG. Chemokines and cell migration in secondary lymphoid organs. Science 1999;286:2098-2102.

21 Sozzani S, Allavena P, Vecchi A et al. Chemokines and dendritic cell traffic. J Clin Immunol 2000;20:151-160.

22 Sozzani S, Allavena P, Vecchi A et al. The role of chemokines in the regulation of dendritic cell trafficking. J Leukoc Biol 1999;66:1-9.

23 Carramolino L, Kremer L, Goya I et al. Down-regulation of the beta-chemokine receptor CCR6 in dendritic cells mediated by TNF-alpha and IL-4. J Leukoc Biol 1999;66:837-844.

24 Yang D, Howard OM, Chen Q et al. Cutting edge: immature dendritic cells generated from monocytes in the presence of TGF-beta 1 express functional C-C chemokine receptor 6. J Immunol 1999;163:1737-1741.

25 Palucka KA, Taquet N, Sanchez-Chapuis F et al. Dendritic cells as the terminal stage of monocyte differentiation. J Immunol 1998;160:4587-4595.

26 Jonuleit H, Kuhn U, Muller G et al. Pro-inflammatory cytokines and prostaglandins induce maturation of potent immunostimulatory dendritic cells under fetal calf serum-free conditions. Eur J Immunol 1997;27:3135-3142.

27 von Andrian UH, Mackay CR. T-cell function and migration. Two sides of the same coin. N Engl J Med 2000;343:1020-1034.

28 Openshaw P, Murphy EE, Hosken NA et al. Heterogeneity of intracellular cytokine synthesis at the single-cell level in polarized T helper 1 and T helper 2 populations. J Exp Med 1995;182:1357-1367.

29 Tao X, Constant S, Jorritsma P et al. Strength of TCR signal determines the costimulatory requirements for Th1 and Th2 $CD4^+$ T cell differentiation. J Immunol 1997;159:5956-5963.

30 Mosca PJ, Hobeika AC, Clay TM et al. A subset of human monocyte-derived dendritic cells expresses high levels of interleukin-12 in response to combined CD40 ligand and interferon-gamma treatment. Blood 2000;96:3499-3504.

31 Tanaka H, Demeure CE, Rubio M et al. Human monocyte-derived dendritic cells induce naïve T cell differentiation into T helper cell type 2 (Th2) or Th1/Th2 effectors. Role of stimulator/responder ratio. J Exp Med 2000;192:405-412.

32 Lee SP, Tierney RJ, Thomas WA et al. Conserved CTL epitopes within EBV latent membrane protein 2: a potential target for CTL-based tumor therapy. J Immunol 1997;158:3325-3334.

33 Zou W, Borvak J, Marches F et al. Macrophage-derived dendritic cells have strong Th1-polarizing potential mediated by beta-chemokines rather than IL-12. J Immunol 2000;165:4388-4396.

Nucleic Acids Research, 1998, Vol. 26, No. 7 1769–1774

Specific tandem GG to TT base substitutions induced by acetaldehyde are due to intra-strand crosslinks between adjacent guanine bases

Tomonari Matsuda*, Masanobu Kawanishi, Takashi Yagi[1], Saburo Matsui and Hiraku Takebe[1]

Research Center for Environmental Quality Control, Kyoto University, 1-2 Yumihama, Otsu, Shiga 520, Japan and [1]Department of Radiation Genetics, Faculty of Medicine, Kyoto University, Yoshida-Konoecho, Sakyo-ku, Kyoto 606-01, Japan

Received November 12, 1997; Revised and Accepted February 10, 1998

ABSTRACT

Acetaldehyde is present in tobacco smoke and automotive exhaust gases, is produced by the oxidation of ethanol, and causes respiratory organ cancers in animals. We show both the types and spectra of acetaldehyde-induced mutations in *supF* genes in double- and single-stranded shuttle vector plasmids replicated in human cells. Of the 101 mutants obtained from the double-stranded plasmids, 63% had tandem base substitutions, of which the predominant type is GG to TT transversions. Of the 44 mutants obtained from the single-stranded plasmids, 39% had tandem mutations that are of a different type than the double-stranded ones. The GG to TT tandem substitutions could arise from intra-strand crosslinks. Our data indicate that acetaldehyde forms intra- as well as inter-strand crosslinks between adjacent two-guanine bases. Based upon the following observations: XP-A protein binds to acetaldehyde-treated DNA, DNA excision repair-deficient xeroderma pigmentosum (XP) cells were more sensitive to acetaldehyde than the repair-proficient normal cells, and a higher frequency of acetaldehyde-induced mutations of the shuttle vectors was found in XP cells than in normal cells, we propose that the DNA damage caused by acetaldehyde is removed by the nucleotide excision repair pathway. Since treatment with acetaldehyde yields very specific GG to TT tandem base substitutions in DNA, such changes can be used as a probe to identify acetaldehyde as the causal agent in human tumors.

INTRODUCTION

Acetaldehyde, one of the most common organic substances used in industry, is the raw material for such products as acetic acid, dyes, photographic chemicals, antioxidants, plastics and synthetic rubber (1). Acetaldehyde has been detected in many foods and in automotive exhaust gases (2). It is present in cigarette smoke, 0.8–1.4 mg acetaldehyde being produced per cigarette (3). Human exposure to acetaldehyde also is common due to the consumption of alcoholic beverages, because it is produced by the oxidation of ethanol. Acetaldehyde produces inter-strand cross-links in calf-thymus DNA *in vitro* (4). It also induces sister-chromatid exchanges in bone-marrow cells of rodents (5,6) exposed *in vivo* and in cultured human lymphocytes (7), as well as chromosomal aberrations in rat embryos (8) and mutations in cultured human skin fibroblasts (9). Inhalation of acetaldehyde causes adenocarcinomas and squamous-cell carcinomas in the nasal mucosa of rats, and laryngeal carcinomas in hamsters (2). Recently, some DNA adducts induced by acetaldehyde were identified. Acetaldehyde reacts with guanine, cytosine and adenine, but not with thymine. Acetaldehyde induces Schiff's base at exocyclic aminogroups of the guanine. The Schiff's base can be reduced by glutathione and ascorbic acid in cells, to form the stable N^2-ethyl-guanine (10). The level of this adduct in lymphocyte DNA of alcoholic patients was 2.1 ± 0.8 adducts/10^7 nucleotides (11). Although acetaldehyde seems to be related to the development of the human tumor, its mutation spectrum is not well known. In this report we present data showing that the predominant types of mutations induced in acetaldehyde-treated shuttle vector plasmids are tandem mutations. We will attempt to elucidate the mechanism for the production of such mutations and its possible biological significance.

MATERIALS AND METHODS

Cells

SV-40 transformed human fibroblast cell lines WI38-VA13 and XP2OS(SV) were used. All cells were cultured in Dulbecco's modified minimum essential medium supplemented with 10% fetal bovine serum.

Chemicals

Biochemicals were obtained from Wako (Kyoto, Japan) except where stated otherwise. Oligodeoxyribonucleotides were synthesized by Nippon Seihun Co. (Tokyo, Japan). pBluescript KS(–) were purchased from Toyobo Co. (Tokyo, Japan). Dynabeads M-280 streptavidin were obtained from DYNAL A.S. (Oslo, Norway).

Shuttle vector plasmid

The shuttle vector plasmid pMY189 was constructed previously by us (12). This plasmid has the *supF* suppressor tRNA gene as

*To whom correspondence should be addressed. Tel: +81 775 27 6224; Fax: +81 775 24 9869; Email: matsuda@biwa.eqc.kyoto-u.ac.jp

an indicator of mutation and replicates in both human and *Escherichia coli* cells. Single-stranded pMY189 was prepared using M13-derived helper phage VCSM13. *Escherichia coli* JM105 containing the pMY189 was infected with the phage in 2× TY medium. After an 8 h incubation at 37°C, the phage was harvested and the single-stranded pMY189 plasmids were purified with QIAGEN M13 Kit (QIAGEN Inc, Chatsworth, CA).

Treatment of plasmids with acetaldehyde and transfection to human cells

Double- and single-stranded pMY189 plasmids (80 µg/ml in TE buffer) were treated with various concentrations of acetaldehyde at 37°C for 1 h. The plasmids were precipitated with ethanol to remove non-reacted excess acetaldehyde, and then redissolved in TE buffer (pH 8). WI38-VA13 cells (2×10^7) transfected with 14.4 µg of the acetaldehyde-treated pMY189 by electric pulses were incubated at 37°C for 72 h in a CO_2 incubator.

Plasmid recovery, selection of mutated supF and DNA sequencing

The plasmids were extracted from the cells and digested with the restriction endonuclease *DpnI* to eliminate non-replicated input plasmids with the bacterial methylation pattern. Plasmid DNA was introduced into the indicator bacteria *E.coli* KS40/pKY241 (12,13) by electro-transformation. The bacteria were spread on LB agar plates containing 50 µg/ml nalidixic acid, 150 µg/ml ampicillin and 30 µg/ml chloramphenicol, together with IPTG and X-gal. Plasmids with mutated *supF* genes made *E.coli* cells resistant to nalidixic acid, whereas cells carrying plasmids with unmutated *supF* genes could not grow in the presence of nalidixic acid. IPTG and X-gal were added to confirm selection of the mutated *supF* gene by the color of the colonies. A portion of the bacteria was spread on plates containing ampicillin and chloramphenicol to measure the transformant fraction and plasmid survival.

Mutated plasmids were extracted and purified from the overnight culture and the base sequences of the *supF* gene of the plasmids were determined with the –21M13 primer and Dye-Primer Cycle Sequencing reagent Kit by the 370A automatic DNA sequencer (Applied Biosystems Foster, CA).

Intra-strand DNA crosslink assay

The sequences of primers and oligonucleotides used in this assay and the scheme of the assay are shown in Figure 3A. The 175 bp region of pBluescript KS(–) was amplified by PCR using primers 1 and 2 (Fig. 3A). Primer 1 was 5′-biotinylated. Approximately 14 pmol of PCR products were bound to the Dynabeads M-280 streptavidin by conjugation between biotin and streptavidin. The PCR products bound to the Dynabeads were denatured with 0.1 M NaOH, collected using a magnet, washed several times with 0.1 M NaOH and then washed twice with TE buffer containing 1 M NaCl, resulting in single-stranded 175mer DNA bound to the Dynabeads. Three kinds of oligonucleotides, oligo 1, oligo 3 and oligo 5, were 5′-labeled with ^{32}P. The labeled oligo 1 and unlabeled oligo 2 were annealed to the single-stranded 175mer DNA by heating and cooling in 1 M NaCl, to detect intra-strand crosslinks between adjacent guanine bases. Oligo 3 and oligo 4, or oligo 5 and oligo 6 were also annealed to the single-stranded 175mer DNA to detect CC- or GC-intra-strand crosslinks, respectively. The annealed DNA (1 pmol of each) was treated with 2 M of acetaldehyde in 0.1 M NaCl for 48 h at 4°C. After collecting the DNA with a magnet, the DNA was dissolved in 10 µl of 0.1 M NaCl. Then, 2 µl of loading buffer consisting of 50% urea, 15% glycerol, 0.25% bromophenol blue (BPB) and 0.25% xylenecyanol (XC) was added to 2 µl of the DNA solution and the samples were subjected to electrophoresis on 12% polyacrylamide gel (50% urea, 1× TBE) for 45 min. at 500 V, and the gel was analyzed by autoradiography.

Cell survival assay

Sensitivity of human cells to acetaldehyde was assayed by colony-forming ability after treatment. An appropriate number of the cells were seeded onto 100 mm Petri dishes and incubated. The next day, the medium was removed and cells were washed with phosphate-buffered saline. After the cells were treated with various concentrations of acetaldehyde for 1 h in a CO_2 incubator, the dishes were washed and refilled with the medium and incubated further until colonies appeared. After fixing and staining, colonies were scored.

XP-A protein binding assay

Nitrocellulose filter-binding assays were performed as described by Robins *et al.* (14) with some modifications. The purified XP-A protein was a kind gift of Dr Kiyoji Tanaka, Osaka University. A *NotI*-digested pBluescript SK(–)-based plasmid (4 kb), labeled with [α-^{32}P]dCTP by Klenow fragment, was used as a DNA probe. The DNA was extracted with phenol, precipitated with ethanol and resuspended in water. The labeled DNA was treated with acetaldehyde (0, 0.5 and 1 M, respectively) for 1 h at 37°C, then precipitated with ethanol and resuspended in water. Binding reaction mixture contained 1 ng of DNA (10 000 c.p.m.) in 50 µl of 20 mM HEPES–KOH pH 7.7, 50 mM KCl, 5 mM $MgCl_2$, 1 mM DTT, 100 µg/ml bovine serum albumin (BSA), 10% glycerol and XP-A protein. After the mixture was incubated for 30 min at 4°C, a 50 µl aliquot was applied to alkali-pretreated nitrocellulose filters (Millipore HAWP 02500, 0.45 µm pore size) and rinsed twice with 0.5 ml of binding buffer without BSA. The residual radioactivity of the filters was counted using a liquid scintillation counter.

Statistics

Statistical comparisons were performed with Fisher's extract test for differences in proportions (15). The *P* values for a one-tailed test are presented.

RESULTS

Mutation induction by acetaldehyde in shuttle vectors replicated in human cells

Acetaldehyde treatment of both the single- and double-stranded pMY189 plasmids increased the frequency of mutation in the *supF* gene on shuttle vectors propagated in normal human cells (Table 1). The background plasmid mutation frequencies were 79 and 1.3×10^{-4} with the single- and double-stranded plasmids, respectively. At 1 M of acetaldehyde treatment, the mutation frequencies of single- and double-stranded DNA were increased to 986 and 54×10^{-4}, respectively.

Table 1. Mutation frequency of acetaldehyde-treated single- and double-stranded plasmids pMY189 propagated in human fibroblasts

Concentration of acetaldehyde (M)	Single-stranded DNA No. of colonies Mutant	Total	Mutation frequency ($\times 10^{-3}$)	Double-stranded DNA No. of colonies Mutant	Total	Mutation frequency ($\times 10^{-4}$)
0	159	20 212	7.9	33	264 000	1.3
0.25	199	11 391	17.5			
0.5	77	2262	34.0	65	48 000	13.6
1.0	35	355	98.6	16	2961	53.7
2.0	21	777	270.3			

Table 2. Type of mutations in the *supF* gene in acetaldehyde-treated shuttle vector plasmids pMY189

Type of mutation	No. of plasmids with base changes (%) double strand	single-stranded
Single base substitution	24 (24)	20 (45)
Base changes including tandem base substitution	63 (62)[a]	17 (39)
Deletion	4 (4)	2 (5)
Insertion	1 (1)	0 (0)
Others	9 (9)	5 (11)
Total	101 (100)	44 (100)

[a]$P < 0.02$ versus single-stranded.

Types and spectra of mutations induced by acetaldehyde in the *supF* gene

Base sequence analysis of mutant plasmids (Table 2) showed that 62% (double-stranded) and 39% (single-stranded) of the mutated plasmids had tandem base substitutions. Tandem mutations were significantly more frequent with double-stranded ($P = 0.007$) than with single-stranded. The distribution of the base substitutions in the *supF* gene is shown in Figure 1 (double-stranded). Tandem base substitutions are present at various sites throughout the gene. While the spectrum of base substitution of single-stranded *supF* gene (Fig. 2) is quite different from that of the double-stranded gene, there is a clear hot-spot involving bases 126–127 in the single-stranded *supF* gene. The types of single base substitutions are listed in Table 3. The predominant types of the mutations are G:C to C:G (54.2%) and G:C to T:A (37.5%) transversions in double-stranded shuttle vectors, while in the single-stranded shuttle vector, G to T (40%) and C to G (20%) mutations are predominant, whereas C to A (15%) and G to C (0%) mutations are minorities. These results suggest that DNA damage induced by acetaldehyde in guanine bases may contribute to the G:C to T:A mutations and damage induced in cytosine bases may contribute to the G:C to C:G transversions. Table 4 shows the types of tandem base substitutions (double strand). Eighty percent of the tandem base substitutions are located at CC (GG) sites, 14% at 5′-GC-3′ sites, and 5% at 5′-CG-3′ sites. The predominant type of mutation is GG to TT (CC to AA) (61%) transversion, which has been reported only in *cis*-diamminedichloroplatinum(II)-induced mutations (16). While almost all the tandem base substitutions of single-stranded shuttle vectors are located at 5′-GC-3′ sites (94%), the predominant type of mutation, GC to TA (47%), is not found in double-stranded shuttle vectors (Table 5).

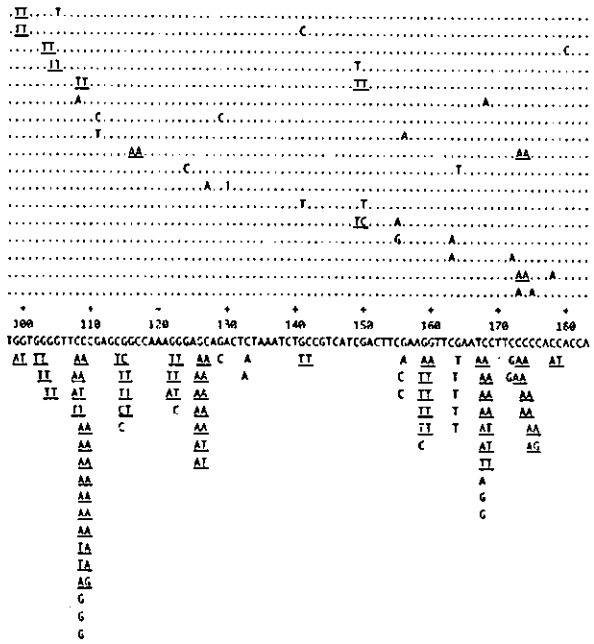

Figure 1. Mutation spectrum of acetaldehyde-treated double-stranded pMY189 replicated in VA13 cells. The location and nature of independent single and tandem (underlined) mutations are indicated below the sequence. The dashed lines above the *supF* sequence represent independent mutants carrying multiple mutations. Several tandem substitutions, present in these multiple mutants, are underlined. Other mutations found in the other region of *supF* gene were as follows; single mutations, G(65) to T and G(72) to A; multiple mutations, large deletion and tandem CC(142, 143) to AA, tandem CC(55, 56) to AA and tandem CC(109, 110) to AA, tandem CC(175, 176) to AA and C(199) to T.

Intra-strand crosslinks induced by acetaldehyde

GG to TT (or CC to AA) tandem base substitutions induced by acetaldehyde may arise from intra-strand crosslinks. To test this hypothesis, the experiment shown in Figure 3 was carried out. If acetaldehyde forms an intra-strand crosslink between ^{32}P-labeled 20mer DNA and non-labeled 20mer DNA, which were annealed to 175mer DNA, a new 40mer band should be detected on the denaturing gel. Figure 3 showed that the 40mer product was detected on the lane where acetaldehyde-treated substrates designated for detection of a GG intra-strand crosslink were loaded, but were not detected on the other lanes. This result indicates that acetaldehyde forms a molecular bridge between adjacent guanine bases and forms little or no intra-strand crosslink between adjacent cytosines nor adjacent guanine and cytosine. Inter-strand crosslinks were also found, which is consistent with earlier findings.